Semiconductor Surface Reconstruction: The Structural Chemistry of Two-Dimensional Surface Compounds

Charles B. Duke

Xerox Wilson Center for Research and Technology, 800 Phillips Road 0114-38D, Webster, New York 14580

Received August 23, 1995 (Revised Manuscript Received November 6, 1995)

Contents

I.	Introduction	1237
II.	Concepts in the Structural Chemistry of Semiconductor Surfaces	1238
III.	Surface Structure Motifs	1239
IV.	Principles of Semiconductor Surface Reconstruction	1241
V.	Elemental Semiconductors	1244
	A. Si(111)	1244
	B. Si(100)	1246
	C. Ge(111)	1247
	D. Ge(100)	1248
VI.	Compound Semiconductors	1249
	A. Zincblende Cleavage Faces	1249
	B. Wurtzite Cleavage Faces	1251
	C. GaAs(111) and ($\bar{1}\bar{1}\bar{1}$)	1252
	D. GaAs(100)	1253
VII.	Synopsis	1256
VIII.	Abbreviations	1256
IX.	Acknowledgments	1256
X.	References	1257

Dr. Charles B. Duke is Senior Research Fellow at Xerox Corporation. Prior to holding this position, he was Deputy Director and Chief Scientist of the Pacific Northwest Division of the Battelle Memorial Institute and Affiliate Professor of Physics at the University of Washington. From 1972 to 1988 he held various technical and management positions at the Xerox Research Laboratories in Webster, NY and was an Adjunct Professor of Physics at the University of Rochester. During 1969–72, he was a Professor of Physics and member of the Materials Research Laboratory and Coordinated Science Laboratory at the University of Illinois in Urbana, IL, following six years as a staff member of the General Electric Corporate Research and Development Center in Schenectady, NY. He received his Ph.D. in physics from Princeton in 1963 following a B.S. *Summa Cum Laude* with distinction in mathematics from Duke University in 1959. He is a Fellow and an Honorary Member of the American Vacuum Society, a Fellow of the American Physical Society, a Fellow of the IEEE, and a life member of Sigma Xi. In 1977, Dr. Duke received the Medard W. Welch Award in Vacuum Science and Technology. In 1979 he served as President of the American Vacuum Society, and since 1979, as Treasurer of its Electronic Materials and Processing Division. He served on the Board of Directors of the American Vacuum Society for seven years. He was chairman of the 1977 Gordon Research Conference on the Chemistry and Physics of Solids and of the 1983 Gordon Research Conference on Organic Thin Films and Solid Surfaces. In 1981 he was named one of the ISI 1000 internationally most cited scientists. During 1985–86 he served as founding editor-in-chief of the *Journal of Materials Research*, the official journal of the Materials Research Society. From 1988 to 1992 and 1995 to 1997, he served (will be serving) on the council of the Materials Research Society, serving as Treasurer during 1991–2. In 1992 he was named editor of *Surface Science*. In 1993 he was elected to the National Academy of Engineering. He is serving on the Council of the American Physical Society during 1995–8. He was chairman of the Board of Editors of the *Journal of Vacuum Science and Technology* during 1976–82 and is currently a member of the editorial boards of *Journal of Materials Research*, *Critical Reviews of Solid-State and Materials Sciences*, *Surface Science Reports*, the *Chemistry and Physics of Surfaces and Interfaces*, and the *Encyclopedia of Applied Physics*. He served on the Governing Board of the American Institute of Physics from 1976 to 1987, being a member of the Board's Executive Committee, Corporate Associates Committee, Educational Policy Committee, Journals Committee, and Committee on Public Education and Information. He has written over 350 papers on surface science, materials research, semiconductor physics, and the electronic structure of molecular solids, as well as a monograph on electron tunneling in solids. He is the editor of *Surface Science: The First Thirty Years*.

I. Introduction

The purpose of this article is to provide an overview of the surface structures of the clean surfaces of tetrahedrally coordinated semiconductors within the context of identifying the main features of their structural chemistry. We develop the point of view that the surface regions of these materials form two-dimensional (2D) compounds whose bonding is constrained by the requirement of epitaxy with the substrate[1] and that the coordination chemistry of these compounds differs from that of molecules or (three-dimensional) bulk solids in specific ways.[2] Our coverage is confined to low-index faces. Specifically, our interest lies in the atomic geometries of ideal single-crystal regions of surfaces rather than in the morphology of surfaces with multiple domains, steps, or defects. Finally, although similar considerations have been applied to interpret oxide surface structures more generally,[3] our attention herein is confined to tetrahedrally coordinated elemental and binary compound semiconductors.

The traditional approach to constructing a review of this type is to consider each surface separately and to describe the structural studies[4−11] or theoretical predictions of surface structure[4−7,12,13] for each individual surface. This procedure offers an abundance of case histories, but little by way of guidance concerning how to make sense out of the wealth of

S0009-2665(95)00212-3 CCC: $25.00

specific results. An alternative approach, pursued sporadically in the literature[12−17] but extended and applied systematically to clean semiconductor surfaces only during the past few years,[2,3] is to extract from the details of specific cases general guidelines, usually referred to as "principles", which govern the behavior of the 2D compounds which form at surfaces. This is the approach which we follow here by first articulating the principles governing the 2D surface structural chemistry and then discussing selected examples in light of these principles.

The coverage of the associated literature is complete on the basis of the author's personal files, augmented by key word computer searches, for the period 1989−94. Prior work is mentioned only if it is of particular historical interest and, where convenient, references to such work are made to the review literature. No effort is made to cite all of the papers on all semiconductor surfaces. We examine selected examples of thoroughly studied low-index faces of elemental or binary compound semiconductors of interest as illustrations of the application of the principles of semiconductor reconstruction. Studies are included in the discussion only if they encompass a quantitative determination or prediction of the microscopic atomic geometry of the surface in question. Thus, this review is an attempt to provide a comprehensible overview of the concepts that govern the reconstruction of semiconductor surfaces rather than a comprehensive listing of papers on any given reconstructed surface. Other reviews in the literature[3−13] already serve the latter purpose. Moreover, compendia of known surface structures also are available.[18−21]

II. Concepts in the Structural Chemistry of Semiconductor Surfaces

Semiconductor surfaces are said to be reconstructed if their symmetry parallel to the surface is lower than that of the bulk solid. A standard notation has been adopted to describe these reduced symmetry structures[22] in which e.g., a Si(hkl)-($n\times m$) symbol designates a structure parallel to the (hkl) lattice plane of Si the dimensions of whose primitive two dimensional unit cell is n times the bulk lattice distance along the x axis and m times it along the y axis. Even if the symmetry of the surface unit cell is the same as that for the bulk, the atoms in the surface region typically move large distances (e.g., tenths of angstroms) relative to the positions which they would have occupied in a truncated bulk lattice. Such surfaces are said to be relaxed (as opposed to reconstructed). We use the term "reconstructed" in the generic sense in this article, without regard to whether the surface symmetry is lowered or not.

Why do semiconductor surfaces reconstruct? Two basic concepts are required to answer this question: chemical bonding and charge neutrality. We can visualize tetrahedrally coordinated semiconductors as being bound together by directional covalent (elemental semiconductors) or partially covalent and partially ionic (compound semiconductors) nearest-neighbor bonds as described e.g., by Pauling[23] or Phillips.[24] These bonds are illustrated schematically in Figure 1 for the diamond and zincblende structure

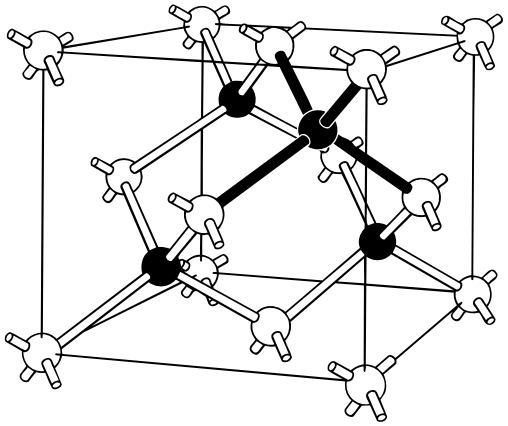

Figure 1. Ball-and-stick model of the zincblende atomic geometry. Open circles represent cations (e.g., Zn) and closed circles anions (e.g., S). If both species are identical (e.g., C, Si, Ge), then this structure becomes the diamond atomic geometry. Balls represent atomic species and lines (i.e., "sticks") the bonds between them. The heavy shadowed lines around the second-layer atom indicate the tetrahedral coordination of the individual atomic species in these structures. (Adapted from Duke, ref 2, with permission.)

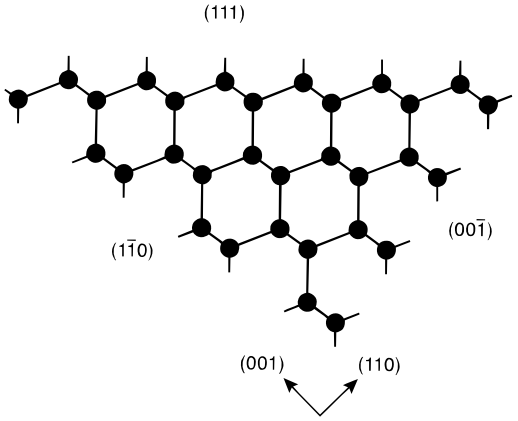

Figure 2. Plane view of a diamond structure elemental semiconductor normal to a (111) plane. Solid circles indicate atoms, and lines indicate bonds. The lines at the surfaces indicate the "dangling" bonds associated with a truncate bulk surfaces. (Adapted from Duke, ref 2, with permission.)

tetrahedrally coordinated semiconductors. Each contains two spin-paired electrons. When a surface is formed, some of these bonds will be broken, leading to associated surface charge densities which contain only one unpaired electron. Such "dangling" bonds are illustrated schematically in Figure 2 for several low index faces. They are unstable. Hence, the atoms in the surface region relax from their bulk positions in order to reduce the surface free energy by forming new bonds. Reaching a structure which exhibits a local minimum in the surface free energy implies that the chemical valencies of the surface species (or at least of most of these species) are satisfied in the reconstructed geometry. For a typical surface multiple local minima, associated with different surface structures, occur in the free energy. Thus, more information is required to describe which structure occurs in a given situation. For all of these structures, however, we expect the atomic chemical valencies, suitably expressed for 2D systems, to be satisfied insofar as a suitable topological arrangement of atoms, compatible with the geometry of the

substrate, can be found which permits this satisfaction to occur.

Not only do the surfaces of semiconductors exhibit relaxed atomic positions, but also in general they have a different chemical composition from the bulk, even for clean surfaces. These compositions are governed by the requirement that the surface region be charge neutral.[15,25] This requirement leads to the prediction of certain specific allowed stoichiometries for the surface compounds. Which composition actually occurs depends on the conditions under which the surface was prepared. If the bulk semiconductor is uncharged (i.e., has no space charge region at the surface), then the surface compound is uncharged and the surface is said to be autocompensated. In general a semiconductor exhibits a space charge region, in which case the surface compound contains just enough charge to render the entire space charge region electrically neutral. In this situation, the charge in the surface compound is typically achieved by the generation of charged defects in an otherwise periodic autocompensated structure.[26]

Although the notions of saturated chemical bonding and charge neutrality suffice to illustrate the basic driving forces of semiconductor surface reconstruction, the description of the details of these reconstructions requires the introduction of additional concepts borrowed from chemical kinetics and solid-state physics. For example, in general the surface structure observed depends upon how the surface is prepared. The Si(111) surface affords an illuminating example of this fact: Low-temperature cleavage generates a (2×1) structure which upon heating first becomes a (5×5) and then a (7×7) structure, and upon further heating the surface disorders to give a (1×1) structure.[10,11] Laser annealing generates a (1×1) structure even at low temperatures[10,27] although high-temperature annealing and cooling always generates the (7×7) structure. For compound semiconductors grown by molecular beam epitaxy (MBE) the situation is even more complex because beam fluxes as well as substrate temperature can be varied.[28] Thus, the kinetic accessibility as well as the ground-state free energy plays an important role in determining which of the various possible reconstructions actually occurs under a specified set of preparation conditions.

Another set of concepts required to determine the details of the structures of these 2D surface structures emanates from the extended nature of the electronic wave functions in solids. In the case of the structures of the (110) cleavage faces of III−V, II−VI, and I−VII binary compound semiconductors, local coordination chemistry considerations suffice to rationalize the surface structures of the III−V compounds but not of the II−VI and I−VII materials.[1,5,7] Achieving a coherent description of the structures of the entire family of materials requires adopting an extended (i.e., delocalized) surface state description of the atomic bonding charge densities in the surface region and specifying the minimum free energy condition (i.e., the saturation of the surface valencies) in terms of these delocalized states. Only when this delocalized description is used can the systematics of the structures across the whole family of materials be explained.[5,7] Another important solid-state concept required to understand the details of semiconductor surface structures is that of Fermi surface instabilities.[2,29] Always in one dimension and under certain circumstances in two dimensions metallic states are unstable to the formation of collective electronic ground states (e.g., charge−density−wave or spin−density−wave states) which generate an energy gap at the metallic Fermi energy, i.e., convert the surface-state eigenvalue spectrum from metallic to semiconducting. These collective electronic states often are accompanied by lattice relaxations which change the structure of the surface (Peierls transitions[29]) as occurs, e.g., in the tilting of surface dimers for Si(100)-(2×1).[2,30] Thus, extensions of the local coordination chemistry model of chemical bonding are required in order to provide a coherent, comprehensive description of the surface structures of tetrahedrally coordinated semiconductors.

Finally, because the rehybridized 2D surface compounds do not fit perfectly on their bulk solid substrates, long-range elastic stress and strain fields occur in the vicinity of the surface.[31−33] In certain situations, e.g., Si(100)-(2×1), these long-range fields can exert a decisive effect on the surface morphology due to the presence of a degenerate ground state associated with different orientations of equivalent domains.[31,34] For the clean surfaces of tetrahedrally coordinated semiconductors the energy stored in these fields usually is small (∼0.01 eV/surface atom), however, relative to that obtained from rehybridizing a dangling bond (∼1 eV/atom).[35] Therefore for determining the atomic geometries of the low index surfaces their influence is often negligible. For vicinal stepped surfaces their influence on the step morphology can be substantial,[31,33] but these effects lie beyond the scope of this review.

III. Surface Structure Motifs

Surface structural studies on the low-index faces of clean elemental and binary semiconductors have revealed a variety of unexpected atomic motifs out of which the structures are composed. Compendia of the major ones have been given by Duke.[2] We recapitulate the highlights of these here to set the stage for the articulation of the principles of semiconductor reconstruction which unify the description of the wide diversity of observed motifs.

Zigzag chain structures, roughly analogous to sp^2-bonded *trans*-polyene chains, occur on the surfaces of both elemental and compound semiconductors. Perhaps the best known of these is the unexpected double-layer chain structure found upon low-temperature cleavage of Si, i.e., Si(111)-(2×1)[10,11,36,37] which is shown in Figure 3. The most common example is found in the structure of the (110) cleavage surfaces of zincblende structure compound semiconductors[4−7,11,38] as shown in Figure 4. Another unexpected occurrence is observed on the cation (111) surfaces of III−V compounds. As indicated in Figure 5, a cation vacancy forms, generating three dangling As bonds to accompany the three dangling Ga bonds in the primitive unit cell. The Ga electrons transfer to the As dangling bonds and the whole structure relaxes to form a chain structure like that shown in Figure 4 for the cleavage faces.

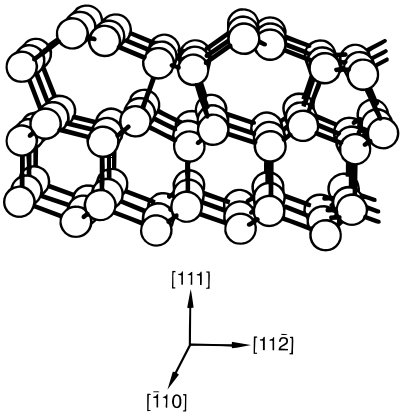

Figure 3. Ball-and-stick model of the (2×1) π-bonded chain structure on Si(111) resulting from the single-bond scission cleavage of silicon. (Adapted from Haneman and Chernov, ref 37b, with permission.)

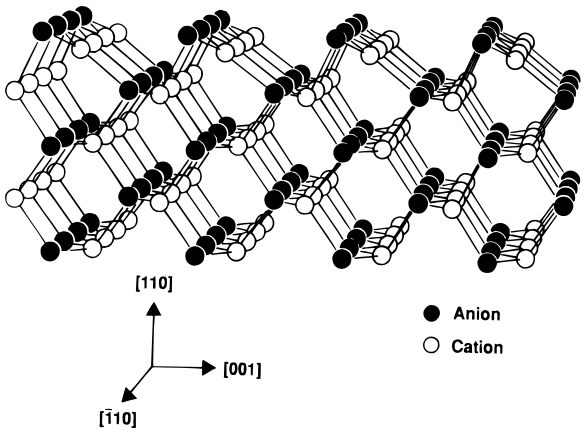

Figure 4. Atomic geometry of the relaxed nonpolar (110) cleavage faces of zincblende structure binary compound semiconductors. (From Duke, ref 7, with permission.)

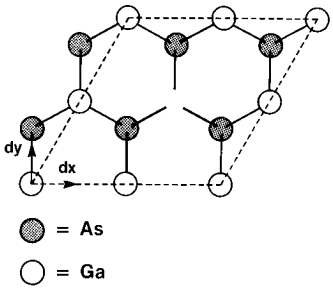

Figure 5. Schematic indication of the ideal (unrelaxed) GaAs(111)-p(2×2)-Ga vacancy structure. (From Duke, ref 9, with permission.)

The energy gained by the relaxation exceeds that required to generate the vacancy, leading to a stable structure predicted by Chadi[39] which has been observed for GaAs,[40] GaP,[41] GaSb,[42] and InSb.[43] A variant of the chain motif is found on the (11$\bar{2}$0) nonpolar cleavage faces of wurtzite structure compound semiconductors.[4−7,38] For these surfaces a glide-plane symmetry does not permit planar zigzag chains, so retention of the appropriate local coordination for the surface atoms produces the puckered chain structure shown in Figure 6. Therefore chain structures constitute a ubiquitous motif on many different types of tetrahedrally coordinated semiconductor surfaces.

A second common motif is a dimer on the surface each of whose constituents is back-bonded to two

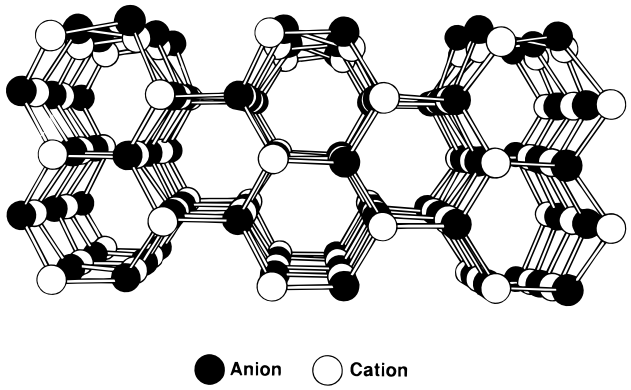

Figure 6. Drawing of the reconstructed ("relaxed") nonpolar (11$\bar{2}$0) cleavage surfaces of wurtzite structure binary semiconductors. (From Duke and Wang, ref 38, with permission.)

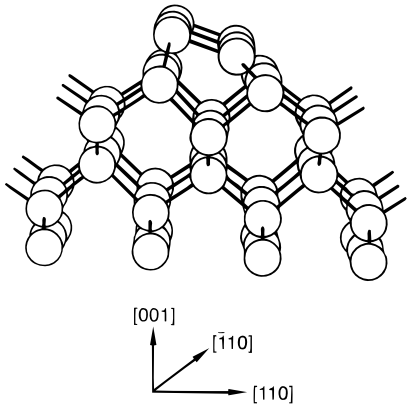

Figure 7. Ball-and-stick model of the buckled dimer structure of Si(100)-(2×1). (Adapted from J. M. MacLauren *et al.*, ref 18. Reprinted by permission of Kluwer Academic Publishers. Copyright 1987.)

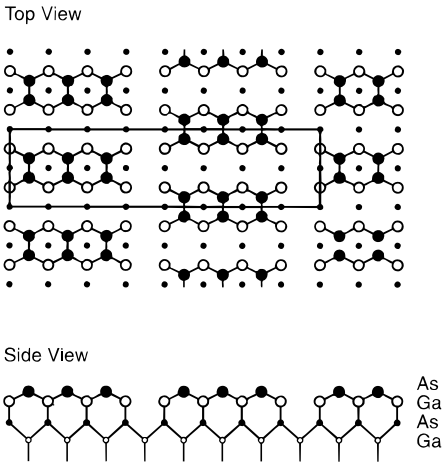

Figure 8. Schematic illustration of the GaAs(100)-c(2×8) [or (2×4)] reconstruction. Dashed lines indicate the surface unit cell. (Adapted from Biegelsen *et al.*, ref 45b, with permission.)

substrate species. Well-known examples include the tilted dimers on Si(100)-(2×1),[8,10−12,30,44] shown in Figure 7 and the variety of dimer and missing dimer structures found on GaAs(100) as a function of preparation condition[4,11,26,45,46] one of which[45] is shown in Figure 8. Contrary to Si(100)-(2×1), the dimers on GaAs(100) are thought to be untilted.[47] Tilted dimers also are found, however, on the (10$\bar{1}$0) cleavage surfaces of wurtzite structure compound semiconductors,[4−7,38] as shown in Figure 9. Thus,

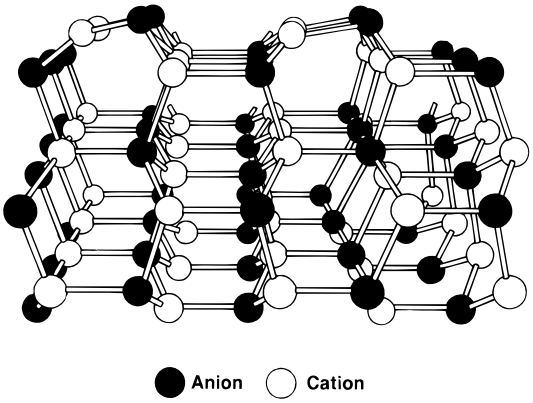

Figure 9. Drawing of the reconstructed ("relaxed") nonpolar ($10\bar{1}0$) cleavage surfaces of wurtzite structure binary semiconductors. (From Duke and Wang, ref 38, with permission.)

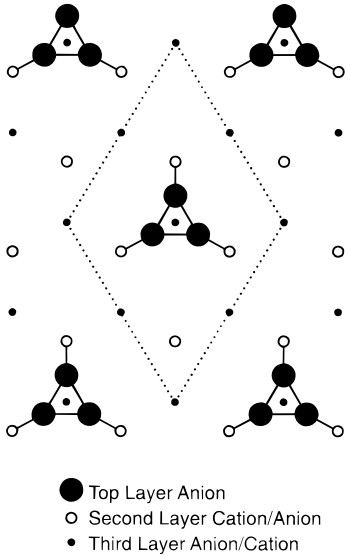

Figure 10. Schematic illustration of the trimer model of the GaAs(111)-(2×2) and GaAs($\bar{1}\bar{1}\bar{1}$)-(2×2) reconstructions. Large solid circles denote top layer As atoms in the "trimer". For GaAs(111)-(2×2) small open circles designate top-layer Ga atoms, and small solid circles denote second layer As atoms. For GaAs($\bar{1}\bar{1}\bar{1}$)-(2×2) small open circles designate top-layer As atoms, and small solid circles denote second-layer Ga atoms. (Adapted from Biegelsen *et al.*, ref 48, with permission.)

dimer structures are found on the surfaces of elemental semiconductors as well as on both the polar and nonpolar surfaces of compound semiconductors.

Trimer motifs seem less common. Thus far, they have only been found on the ($\bar{1}\bar{1}\bar{1}$) surfaces of GaAs.[11,48] A schematic diagram of the possible trimer structures is given in Figure 10.

Two additional motifs are observed on the surfaces of elemental semiconductors: 3-fold coordinated adatoms and stacking faults. Both are observed on the Si(111)-(7×7) structure[8,10,11,49] shown in Figure 11. The 3-fold coordinated adatoms also are a prominent feature of the Ge(111)-(2×8) structure.[11,50] The Si(111)-(7×7) structure also exhibits dimers and 3-fold coordinated substrate atoms ("rest" atoms).

Figures 3−11 illustrate well the range of structural motifs and behaviors observed at the low-index surfaces of tetrahedrally coordinated semiconductors. In the literature, each surface is typically considered as a special case, complete with its own history and story of changing opinions about the "correct" structure as a function of time. Our goal here is to alter this case-by-case perspective and, instead, to examine the entire structural and theoretical information base to extract generalizations which describe the systematics of the observed structures. Thus, in the following section we propose five "principles" which describe most, if not all, of the structures observed to date. Application of these principles will enable the interpretation of most of the observed features in a straightforward way, and offer considerable predictive powers in new cases. In some situations, e.g., the cleavage faces of binary compound semiconductors, even more powerful scaling laws and universality principles may apply.[2,7] In others, e.g., the determination of surface morphology, additional considerations like surface stress need to be added. The principles form, however, a useful base from which to view the wide variety of experimental and theoretical results in order to appreciate the significance of the entire scope of the results, as well as the specific details of each individual case.

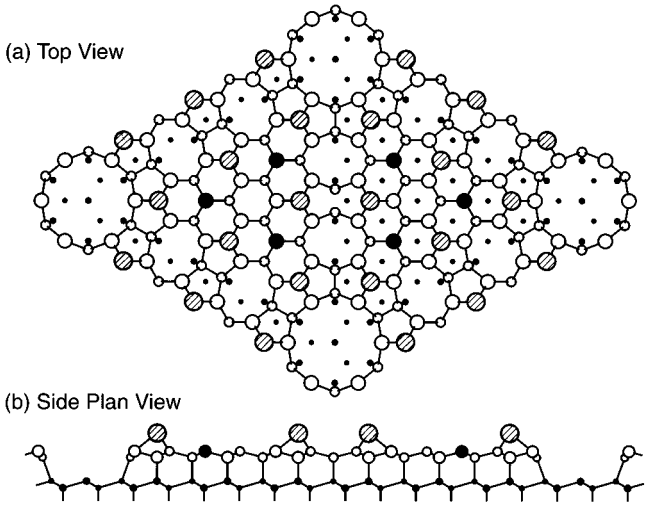

Figure 11. Schematic illustration of the top (panel a) and side (panel b) views of the dimer−adatom−stacking−fault (DAS) model of the Si(111)-(7×7) structure. The side view is given along the diagonal of the unit cell. In the top view (panel a) the large striped circles designate the adatoms in the top layer of the structure. The large solid circles designate "rest atoms" in the second layer which are not bonded to an adatom. Large open circles designate triply bonded atoms in the layer, whereas small open circles designate 4-fold coordinated atoms in the bilayer beneath. Smaller solid circles designate atoms in the fourth and fifth bilayer from the surfaces. The size of all circles is proportional to the proximity to the surface. The side view (panel b) is a plane view of the nearest-neighbor bonding in a plane normal to the surface containing the long diagonal of the surface unit cell. Smaller circles indicate atoms out of the plane of this diagonal. (Adapted from Takayanagi *et al.*, ref 49, with permission.)

IV. Principles of Semiconductor Surface Reconstruction

In order to construct a synthetic view of the driving forces of semiconductor reconstructions, it is useful to regard the surface region as a new chemical compound whose structure and composition is constrained by the fact that it must fit epitaxically on the corresponding bulk substrate.[1,2] These compounds correspond to minima in the surface free energies, so their structure and properties may be evaluated theoretically by minimizing the free

energy.[12,13,35] Multiple minima occur for most surfaces, differing in both composition and structure. Which minimum is accessed experimentally depends upon how the surface is prepared. Thus, a typical surface exhibits multiple structures depending upon preparation conditions as well as on the ambient temperature and pressure. Finally, these structures and their properties are characteristic of two-dimensional (2D) systems of finite thickness. In order to describe their structure and bonding we need to utilize concepts appropriate to the description of extended 2D systems, as indicated in section III. In particular, the development of suitable concepts requires extensions of those used describing the local coordination chemistry of molecules and adaptations of those used in describing that of bulk (three-dimensional) solids.[2]

Our approach to developing a synthetic view of semiconductor surface reconstruction is to search the literature for general features of semiconductor surface structures and their interpretation which can be abstracted as "principles" which describe their construction. This sort of activity has a long history, indicated with varying degrees of explicitness in several of the reviews cited.[2,6,8,12,13,25] Building on earlier work, Duke[2,51] proposed an explicit set of five principles suitable to describe the clean low-index faces of tetrahedrally coordinated elemental and compound semiconductors. These principles are built on two important foundations, the concepts of 2D chemical bonding and the charge neutrality of surfaces, as described in section III. In the simple cases that we consider, no space charge occurs so the surface compounds are electrically uncharged, i.e., autocompensated. In this limit, the five principles of semiconductor surface reconstruction for the surfaces of tetrahedrally coordinated compound semiconductors can be articulated as specified in the remainder of this section.

Principle 1: Reconstructions tend either to saturate surface "dangling" bonds via rehybridization or to convert them into nonbonding electronic states.

This principle, as stated, applies to group IV semiconductors. Extensions are required for compound compounds.[5,7,12] Suitable extensions appropriate for all tetrahedrally coordinated compound semiconductors (III−V, II−VI, and I−VII) are given as principles 4 and 5 below. If epitaxy with the substrate permits chemically sensible 2D surface compounds satisfying this requirement to exist, they occur. Sometimes, for example the (111) surfaces of Si and GaAs, structures which rigorously satisfy this requirement contain so much strain or coulomb repulsion between distorted bonds that lower symmetry structures which only partially satisfy it may exhibit lower free energies. Even in these cases, however, the energetics of the resulting structures may be described in terms of models which express the idea that they minimize the number of dangling bonds.[8,52] Thus, the notion of forming surface compounds comprised of atomic species with satisfied surface valencies is a fundamental principle which spans the numerous special cases of tetrahedrally coordinated semiconductor surface structures.

Principle 2: In many cases (and in all quasi-one-dimensional ones) surfaces can lower their energies by atomic relaxations leading to semiconducting (as opposed to metallic) surface state eigenvalue spectra.

This principle expresses the result that in systems with extended electronic wave functions, metallic ground states do not occur in one dimension (1D) and in certain circumstances also do not occur in two dimensions (2D).[29] Perhaps the clearest example of its operation on tetrahedrally coordinated semiconductor surfaces is the tilting of the dimers on Si(100) and Ge(100).[30,44] If the dimers were untilted, the occupied and unoccupied π bands associated with the surface dimers would overlap, and the chains of dimers along the surface would form a semimetal. As noted above, semimetals are unstable in 1D and in this case the resulting collective ground state is characterized by a Peierls distortion of the dimers. The applicability of this principle to semiconductor surface structures is an example of the result that the properties and energetics of these structures are governed by principles which describe systems which exhibit extended electronic states in one or more dimensions. That is, local coordination chemistry considerations alone are inadequate to account for all of the observed properties of semiconductor surface structures.

Principle 3: The surface structure observed will be the lowest free-energy structure kinetically accessible under the preparation conditions.

As noted earlier, in general the structure observed on a semiconductor surface will depend on the process used to prepare the surface. This is hardly surprising: Essentially all of the structures utilized in semiconductor electronic devices are metastable at room temperature and are designed to be produced with a sequence of process steps chosen so that the results of earlier steps are not damaged by subsequent ones. Metastable structures need not be the consequence of minima in the free energy, however, whereas the semiconductor surface structures which we discuss here do correspond to free energy minima. This is reflected in the fact that they may be generated by a variety of process conditions and correspond, therefore, to a local (but not necessarily the global) minimum in the free energy. This principle captures the result that the observed structure is that corresponding to the lowest free-energy minimum which can be reached kinetically by the process conditions used to prepare the surface.

The clearest examples of the operation of this principle are the (111) cleavage faces of Si and Ge. Low-temperature cleavage produces a (2×1) structure, whereas annealing to high temperatures produces the Si(111)-(7×7)[10,11] and the Ge(111)-c(2×8)[11,53] both of which are stable upon subsequent cooling. A diagram of the Ge(111)-c(2×8) structure is given in Figure 12.[54] At still higher temperatures both surfaces exhibit a (1×1) structure before the bulk crystal melts,[10,11,55] sometimes reaching the final high-temperature structure in more than one stage.[11,55] The (2×1) structure obtained by low-temperature cleavage is a locally stable structure, but not the lowest free-energy structure which is obtained for both surfaces by annealing and subsequent cooling, high temperatures being necessary to generate the adatoms in the lowest free-energy structures.

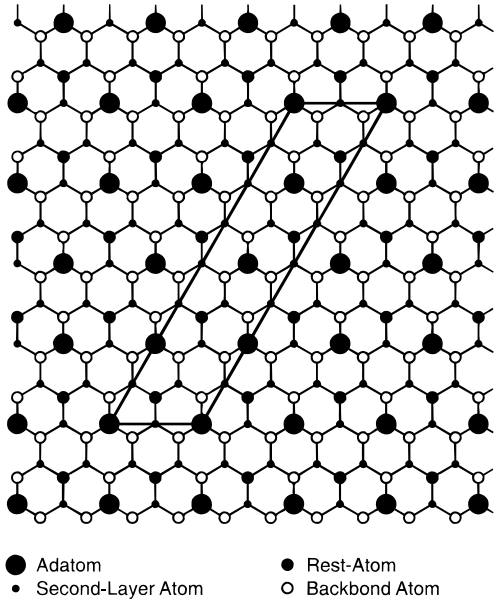

Figure 12. Schematic illustration of the top view of the adatom model of the Ge(111)-c(2×8) low-temperature equilibrium structure. The adatoms, top-layer atoms bonded to adatoms ("back-bond atoms"), top-layer atoms not bonded to an adatom ("rest atoms") and second-layer atoms are indicated. (From Klistner and Nelson, ref 54, with permission.)

Principles 1−3 are the only ones required for space−charge free elemental semiconductors, but for compound semiconductors the surface atomic composition may be different from that of the bulk and large charge transfer routinely occurs at the surface from one atomic species to another. Describing these phenomena requires an additional principle to specify the outcome of the charge transfer and a reformulation of principle 1 to comprehend structural scaling relations between III−V, II−VI, and I−VII compound semiconductors. In the form in which we present these two principles they encompass principle 2 as well in that applied in combination they automatically generate semiconducting surface state spectra. Thus, for compound semiconductors principles 1−3 are replaced by principles 3−5 where principles 4 and 5 are specified as follows:

Principle 4: Surfaces tend to be autocompensated.

An important constraint which limits the possible stoichiometries of compound semiconductor surfaces is the requirement that no charge accumulate at the surface.[15] In the limit that surface defects which account for the compensation of charge in the space charge layer are neglected, the surface is electrically neutral. In this limit, the charge neutrality constraint has been developed into a set of electron-counting rules which can be applied directly to determine allowable surface compositions.[25,56] These rules are based on the hypothesis that bonding and nonbonding surface states that lie below the Fermi energy at the surface must be filled, whereas the nonbonding and antibonding states which lie above this energy must be empty. This criterion is labeled the "nonmetallicity" condition. As noted above, it encompasses principle 2 in that surface relaxations must occur to insure the validity of this condition. Surfaces which satisfy it are said to be autocompensated. In order to deal with doped semiconductor these rules must be extended to account for defects at the surface which compensate the space charge.[26] In this extended form, the autocompensation principle is satisfied by all known structures for which a quantitative test is available. It has been proposed to fail for only one structure:[48] GaAs($\bar{1}\bar{1}\bar{1}$)-($\sqrt{19}$x$\sqrt{19}$) which is a complex structure for which neither a detailed structure analysis nor a description of the surface bonding is yet available.

This principle describes a wide variety of structures on the polar surfaces of compound semiconductors.[25,26,45,46,48,56−59] It is satisfied identically on the nonpolar cleavage faces of compound semiconductors. For the polar surfaces, it specifies a set of allowed stoichiometries, and hence candidate structures, from which the actual structure can be selected by experimental determination. For example it predicts the 3:1 ratio of anion dimers to missing anion dimers shown in Figure 8 or a corresponding structure in which one of the dimers occurs in the third layer;[45] the 2:2 ratio of top-layer anion dimers to second-layer cation dimers which occurs when the second layer also dimerizes,[46] the change to a uniform (2×1) dimer structure on II−VI(100) as opposed to missing dimer structures on III−V(100),[56d] and the further change to a c(2×2) anion or cation vacancy structure on I−VII(100).[58] It also describes the III−V(111)-(2×2) cation vacancy structure shown in Figure 5[40−43] and the III−V($\bar{1}\bar{1}\bar{1}$)-(2×2) anion trimer structure shown in Figure 10.[48] Detailed microscopic calculations also support its validity,[56a,60] so its viability and utility are firmly established.

Principle 5: For a given surface stoichiometry, the surface atomic geometry is determined primarily by a rehybridization-induced lowering of the surface state bands associated with either surface bonds or (filled) anion dangling bond states.

Whereas for compound semiconductors principle 4 determines allowed surface stoichiometries, principle 5 determines their detailed atomic geometries. It is formulated as an extension to compound semiconductors of principle 1 which as articulated is most useful for the nonpolar surfaces of group IV and III−V semiconductors. Principle 5 is an extension of principle 1 for both nonpolar and polar surfaces because it embodies a new notion not contained in principle 1: that of surface chemical bonding carried by the delocalized electronic surface states characteristic of a two-dimensional epitaxically constrained surface compound. This is an extension of traditional local bonding concepts characteristic of molecular bonding[61] and bulk solid[23] bonding which is required to comprehend the similarities between the cleavage surface bonding of III−V, II−VI, and I−VII semiconductors.[1,7] Thus, principle 5 can be applied to describe the relaxations of the cleavage faces of II−VI and I−VII semiconductors whereas principle 1, while true, does not illuminate the origin of the resulting surface structures. Principle 5 is, moreover, subject to direct experimental verification in that the surface states which carry the surface chemical bonding can be observed directly by angle-resolved photoemission spectroscopy (ARPES). Thus, hypotheses about the character of this bonding can be tested

directly by comparing the predictions of suitable theoretical descriptions of these hypotheses with ARPES results.[5−7,11,12] This aspect of principle 5 is useful in interpreting results for group IV and III−V as well as II−VI and I−VII surfaces.

A major motivation for developing principle 5 as an extension to principle 1 is the recognition[62] that the (110) cleavage surface structures of all zincblende structure compound semiconductors are essentially identical when distances are measured in units of the bulk lattice constant. Since the coordination chemistry of II−VI compounds differs greatly from that of III−V's, local coordination chemistry concepts like those articulated in principle 1 had to be recast into the more general context of principle 5. The verification of principle 5 for the cleavage faces of both wurtzite and zincblende II−VI and III−V compounds has been described by Duke.[7]

For the zincblende cleavage faces, the surface structure scaling rules have been extended to develop a more general notion of universality for the potential energy surfaces governing the relaxation and lattice dynamics of these surfaces.[7,63] The minima in these surfaces specify the relaxed atomic geometries, whereas their curvature in the vicinity of these minima specify the effective atomic dynamics spring constants (and hence the phonon frequencies). The existence of scaling laws predicted by these potential energy surfaces confirms the concept that the constraint of epitaxy with the tetrahedrally coordinated substrate leads to new types of surface chemical bonding, mediated by delocalized two-dimensional surface states rather than by local molecular coordination chemistry. Principle 5 is an expression of this result.

Principle 5 has not been tested rigorously for surfaces other than the zincblende and wurtzite cleavage surfaces. Since the new motifs characteristic of epitaxically constrained surface chemical bonding are localized within a few atomic layers of the surface, their bonding and occupied nonbonding charge densities must, by definition, be comprised of linear superpositions of electronic eigenstates which are surface states or resonances. Energy minimization calculations[8,12,13,30,32,35,36,39,60,64−66] rarely identify the surface-state contributions to the total energy. Hence, the microscopic origin of the energy lowering by virtue of the surface relaxation often is not explored. Only for zincblende[7,67] and wurtzite[38,68] cleavage faces has the separation of the surface state energies been made sufficiently explicit that principle 5 can be validated. Principle 5 is, however, expected to be valid for all surfaces of tetrahedrally coordinated semiconductors, reducing in some cases to principle 1 which is more visualizable in terms of traditional local chemical bonding concepts.[23,61]

These principles can be comprehended only by applying them. Thus, in the following two sections we indicate their application to the interpretation of some extensively studied surface structures. These examples, hopefully, serve to make the principles "real": i.e., directly useful to the reader. The essence of this article, however, is its point of view to toward the topic, which already is articulated in this and the preceding three sections.

V. Elemental Semiconductors

A. Si(111)

Si(111) is the cleavage face of silicon. As noted earlier, low-temperature ($T \leq 600$ K) ultrahigh vacuum (UHV) cleavage produces a (2×1) structure. Annealing this surface to above 603 K (in vacuum) generates a (5×5) structure which upon further heating to 873 K becomes a (7×7) structure.[11] This conversion process is quite complex, depending explicitly upon the process conditions and initial morphology of the Si(111) surface.[11] Still further heating to about 1123 K causes the surface to disorder. A large volume of literature (hundreds of papers) has been generated on these structures and the transitions between them. This literature through mid-1986 has been reviewed by Haneman.[10] Selected aspects have been discussed more recently by Mönch.[11] Our purposes in this section are to examine the extent to which the (2×1) and (7×7) structures satisfy the principles articulated in the preceding section and to indicate the major contributions to the determination and prediction of these structures since Haneman's review. The (5×5) structure is thought to exhibit a structure analogous to that of the (7×7) for which much more extensive quantitative structure determinations have been reported.[10,11]

If the Si crystal is cleaved so that only one bond per Si atom is broken, then the Si(111)-(2×1) structure shown in Figure 3 results. It was first predicted by Pandey[69] and confirmed subsequently by a host of experimental measurements and theoretical predictions.[8,10] Quantitative structure determinations have been performed using low-energy electron diffraction (LEED)[70] and ion scattering.[71] A recent first principles prediction[72] of this structure compares favorably with these results, as do it predecessors.[73] Recent scanning tunneling microscopy (STM) experiments[74] have confirmed both the structure itself and the existence of a gap between the occupied (π) and excited (π^*) pi electron states associated with the tilted chains shown in Figure 3. Moreover, calculated π-electron occupied and empty surface state eigenvalue spectrum show excellent correspondence with the measured photoelectron spectra as demonstrated by Northrup *et al.*[72] and shown in Figure 13. Thus, the acceptability of the structure shown in Figure 3 is well established.

This structure obeys the principles articulated in section IV. Principle 1 is satisfied because all of the valencies of the surface Si species are satisfied: three by bonding σ electrons, shown by the lines in Figure 3, and the final one by the π bonds corresponding to the lower surface state shown in Figure 13. Principle 2 is satisfied because the π and π^* bands shown in Figure 13 do not overlap. The tilting of the surface chains renders neighboring atoms in these chains sufficiently electronically inequivalent to insure a semiconducting surface-state eigenvalue spectrum. Finally, principle 3 is satisfied because the energy barrier for relaxation from the truncated bulk surface to the π-chain structure shown in Figure 3 has been shown to be sufficiently small that this structure is kinetically accessible.[73a] Principles 4 and 5 apply to compound rather than elemental semiconductors. Thus, these principles do indeed "explain" (i.e.,

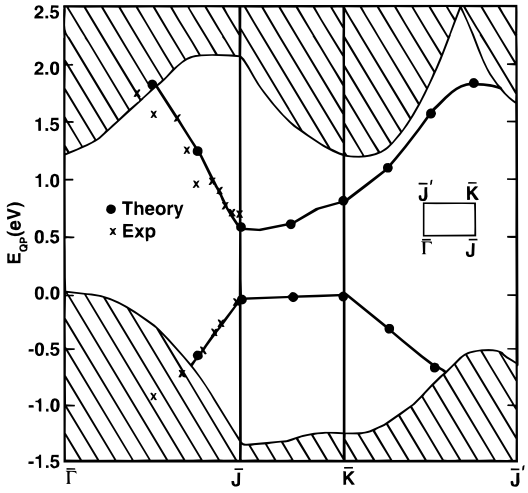

Figure 13. Comparison of the calculated (solid circles) and measured (crosses) electronic surface state eigenvalue spectra for Si(111)-(2×1). The top band is the empty π^* band and the lower one is the occupied π band. The surface Brillouin zone for Si(111)-(2×1) is shown in the inset. (From Northrup, Hybertson, and Louie, ref 72, with permission.)

permit the rationalization of) the Si(111)-(2×1) structure shown in Figure 3.

The only serious challenge to this structure has been raised by Haneman and co-workers[37] who argue that a three bond scission π-chain structure would be equally compatible with the STM measurements, surface-state excitation spectra, and the thermodynamics of surface formation and transformation. Given the quantitative structure analyses and theoretical predictions of the one-bond scission structure shown in Figure 3 this possibility seems a bit remote, although the quality of the fits of the LEED intensity data[70] indicate that a revised analysis could produce a structure which is equally or better correlated with the data. The proposed three bond scission structure is equally compatible with our principles of semiconductor surface reconstruction, so these principles do not distinguish between the two possibilities. Only more structural and theoretical analyses can resolve this issue.

The generally accepted[10] dimer−adatom−stacking−fault (DAS) model of the Si(111)-(7×7) structure is shown in Figure 11. It was proposed on the basis of an analysis of transmission electron diffraction data by Takayanagi *et al.*[49] in 1985 and subsequently has been tested and/or refined by LEED,[75] glancing incidence X-ray diffraction,[76] X-ray reflectivity,[77] transmission electron diffraction,[78] STM,[79] and reflection high-energy electron diffraction (RHEED).[80] This is the most complex and famous clean surface structure in the history of surface science. The lengthy history of attempts at its determination is summarized from two different points of view in the reviews by Schlüter[8] and Haneman.[10] Some discrepancies between the various determinations of the detailed structural coordinates remain (e.g., the height of the adatoms[77]), but the general features of the DAS structure seem well established.

An important recent development is the extension of *ab initio* local density functional (LDF) total energy calculations to run on parallel supercomputers thereby enabling their application to large structures like Si(111)-(7×7).[64] The atomic geometry of the DAS structure has been predicted this way[64a,b] and judged to give an even better description of RHEED data than the original DAS structure and its LEED refinement.[80b,c] These predictions also are in good agreement with an earlier (semiempirical) tight-binding-model calculation[81] of the structure. They permit, moreover, a quantitative comparison of the relative energies of the (2×1) and (7×7) structures (subject to certain technical approximations which accompany any calculation of this nature[64c,d]) which leads to the result that the (7×7) is lower in energy (at zero temperature) by 0.06eV per (1×1) unit cell: a remarkably small number indicative of the many competing phenomena which lead ultimately to this complicated structure.

Naively, the Si(111)-(7×7) structure may not seem to satisfy our principles because its surface electronic excitation spectra is believed to be metallic, indicative of residual unsatisfied valencies at the surface, in contradiction to the spirit (but not the detail) of principle 1. Metallic excitation spectra are not precluded for 2D systems by principle 2, however, so that this principle is satisfied, as is the third because the high-temperature heating of the sample allows adatoms to be generated from the (2×1) surface which then converts in a stepwise fashion into the (7×7).[11,82] As noted above, the (7×7) has been shown explicitly to have the lowest free energy of the plausible structures, at least at zero temperature, so that its generation under suitable kinetic conditions is expected. The concept which we require to comprehend the operation of principle (1) for the (7×7) structure is the saturation of surface valencies by dimer row domain walls between faulted and unfaulted regions of a Si(111) surface. A model which explicitly embodies the tradeoffs between dangling bond removal via adatom decoration and the formation of stacking faults, with their concomitant domain walls between faulted and unfaulted regions of the surface and corner holes at the intersections of these domain walls, has been developed by Vanderbilt.[52] In this model the primary driving force for the surface reconstruction is the elimination of dangling bonds by dimer−row domain walls (which are energetically most favorable) at a cost in energy of the formation of stacking faults and corner holes. Adatom formation merely reduces the effective cost in energy of a corner hole. If the cost of forming the stacking faults and corner holes is too great, simple dangling bond−removing adatom structures are formed, like the c(2×8) structure of Ge(111) shown in Figure 12. If their cost is exceeded by the energy gained by the formation of domain walls, then the conditions of epitaxy on diamond structure (111) surfaces permit a family of (3×3), (5×5), (7×7), etc. structures consisting of faulted and unfaulted regions separated by domain walls. Since strain impacts the costs of the stacking faults and corner holes, the imposition of external strain can cause transitions between the different possible structures. Vanderbilt shows that this model can describe a variety of otherwise puzzling results on the stress dependence of Si(111) and Ge(111) surface structures. In terms of this model, principle 1 is satisfied. The Si(111) surface minimizes its dangling bonds by the forma-

tion of dimer−row domain walls which are energetically favorable because of the relative low energies of stacking fault and corner hole formation. Not all the dangling bonds are removed in this fashion, so a metallic surface state eigenvalue spectrum can result. From this perspective the Si(111)-(7×7) DAS structure is a consequence of the ease of forming stacking faults in Si: a solid-state effect that renders unnecessary the saturation of all the dangling bonds by adatoms in favor of forming ordered epitaxical patterns of solid-state defects at the surface. This phenomenon saturates most of the bonds, and the remaining electrons form nonbonding (or weak π-like bonding) 2D surface state bands, as indicated by principle 1. Therefore the principles of semiconductor surface reconstruction articulated in section IV describe even complicated structures like the Si(111)-(7×7) once the possibilities introduced by the solid-state nature of the substrate are comprehended.

B. Si(100)

As in the case of Si(111), the literature on Si(100) is substantial. Thorough accounts of the work prior to 1987 are given in the reviews by Schlüter[8] and Haneman[10] which are updated in part by Mönch.[11] *Circa* 1987 this surface, prepared by suitably cutting a bulk crystal and subsequently vacuum processing it, was believed to exhibit the (2×1) structure shown in Figure 7. Lower symmetry low-temperature phases had been predicted,[83] and regions of c(4×2) and p(2×2) symmetry had been observed by STM at room temperature.[84] The dimer surface motif was well established by 1987, although debate was occurring as to whether or not the dimers were tilted.[8,10]

The (2×1) dimer structure shown in Figure 7 is in excellent correspondence with the principles articulated in section IV. From a chemical perspective, we can regard the surface dimer in Figure 7 as being bound by a σ bond emanating from the two dangling bond orbitals in between the dimerized surface atoms and a weaker π-like bond emanating from the two dangling bond orbitals pointed away from the dimer. The associated π^* bonding orbital is empty but is separated from the bonding orbital by only a small energy gap ($E_g \sim 0.5$eV).[44] Because of the two-dimensional character of the surface the molecular π and π^* orbitals broaden into bands associated with the wave vectors in the surface Brillouin zone. These bands overlap for a symmetric (i.e., untilted) dimer, so that the surface becomes metallic, as shown in the lower panel of Figure 14. Since these bands are nearly one dimensional (along the rows of dimers), however, in accordance with principle 2, it is energetically favorable for the surface to lower its energy by an atomic relaxation[2,29,30] and hence the dimers tilt, opening up a gap between filled electronic states originating primarily from the "up" atom and empty states originating primarily from the "down" atom. The resulting "asymmetric" or tilted dimer model is in good quantitative accord both with experimental determinations of the surface excitation spectra[85] and with modern (i.e., converged) total energy calculations.[65,66,86] The asymmetric dimers have been observed directly by UHV transmission electron

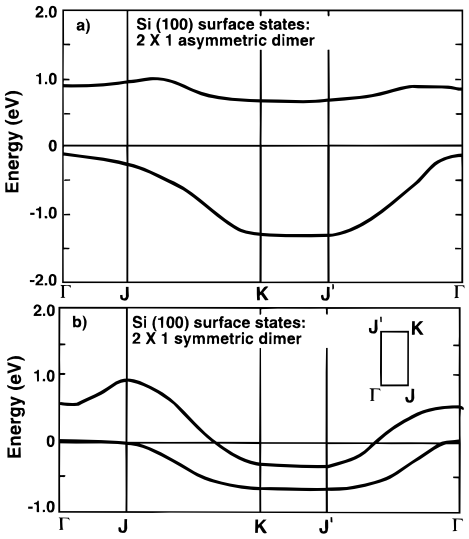

Figure 14. Filled and empty (π and π^* like) surface-state bands associated with tilted (top panel) and symmetric (lower panel) dimers on Si(100)-(2×1). The inset shows the surface Brillouin zone associated with the (2×1) surface unit cell. The lower panel shows that this surface would be metallic if the dimers did not tilt. (From Chadi, ref 44a, with permission.)

diffraction,[87] by analysis of of the differential reflectivity associated with the π and π^* surface states,[88] and at low temperatures by STM.[89] Moreover, the charge asymmetry on the up and down atoms in the dimer has been observed by both STM[90] and high-resolution core level spectroscopy.[91] Thus, both the occurrence and the origin of the asymmetric dimers seems well established.

Subsequent to the most recent two major reviews of Si(100),[8,10] new work has been reported which reveals that the ground state of Si(100) is not a (2×1) state but rather a c(4×2) state in which the dimers are tilted in alternating directions along the dimer rows. A discussion of the theoretical literature on this topic through 1991 may be found in the review by LaFemina.[12] An order−disorder transition from the c(4×2) structure to the (2×1) structure was reported at about 200 K using LEED.[92] This finding was confirmed by direct observation via STM of c(4×2) domains at low temperatures[89] and of the abrupt growth in these domains at about 200 K.[93] The ground-state geometry and surface-state excitation spectra have been calculated by Northrup[94] and compared with the experimental angle-resolved photoemission determination of the surface-state excitation spectra.[95] A schematic diagram of the structure of the c(4×2) structure is shown in Figure 15. A comparison of the calculated[94] and measured[95] surface-state excitation spectra is given in Figure 16. This figure reveals the quantitative correspondence between the calculated and observed bonding π-electron surface-state bands, similar to that reported earlier by Enta *et al.*[96] Numerous other calculations have revealed a preference for the c(4×2) geometry over (2×1) or p(2×2) alternatives.[12,44a,97,98] The alternation of the buckled dimers to form a c(4×2) rather than a (2×1) ground state also is required to give a good description of the measured stress anisotropy at Si-(100) surfaces.[98]

The c(4×2) structure satisfies the principles of semiconductor surface reconstruction. The two bond-

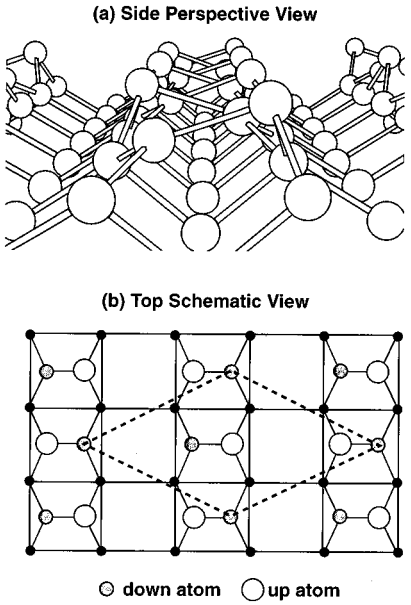

Figure 15. Panel a: Ball and stick model of a row of dimers on the Si(100)-c(4×2) structure. Panel b: Schematic indication of the symmetry of the c(4×2) tilted dimer structure on Si(100). (Adapted from Northrup, ref 94, with permission.)

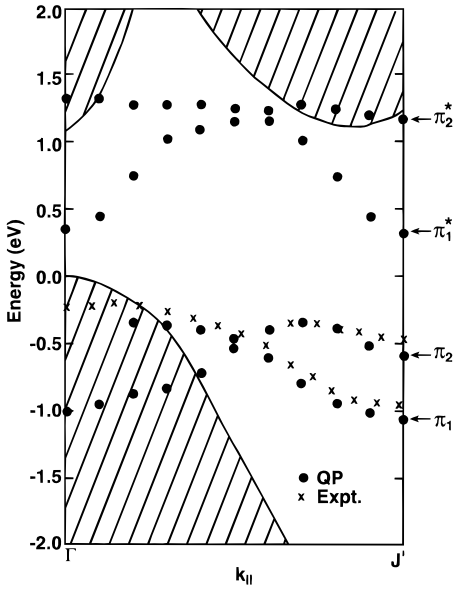

Figure 16. Filled (π) and empty (π^*) surface-state bands associated with the Si(100)-c(4×2) structure illustrated in Figure 15 along a symmetry line in the surface Brillouin zone. Dots indicate calculated surface-state excitation energies and crosses indicate the experimental surface state spectra obtained by Johansson *et al.*[95] The four surface state bands arise from the four "dangling bond" electrons in the c(4×2) surface unit cell. (From Northrup, ref 94, with permission.)

ing π bands plus the three σ bonds (two back bonds, one surface bond) of the four Si atoms in the surface unit cell satisfy their valencies, so principle 1 is satisfied. The tilting of the dimers gives the semiconducting surface state excitation spectra shown in Figure 16 as expected from principle 2. Since the c(4×2) structure is the lowest free energy structure (at $T = 0$), it is expected via principle 3 to be generated from the Si(100) surface under suitable processing conditions. Thus, these principles describe the known structures on Si(100) as well as Si(111).

C. Ge(111)

A recent account of the structure of Ge surfaces has been given by Mönch,[11] although there are no comprehensive reviews of Ge analogous of those for Si.[8,10] We take as the starting point of our literature citations two discussions of the Ge(111) surface in 1985 by LEED[53a] and STM,[53b] respectively.

As in the case of Si(111), room temperature cleavage of Ge(111) results in a 2×1 structure which is believed to be similar to the Si(111)-(2×1) shown in Figure 7. Low temperature ($T \leq 40$ K) cleavage may result in a more complicated structure.[99] Annealing to 600 K and subsequently cooling produces the c(2×8) structure shown in Figure 12.[53] Heating this c(2×8) to about 573 K produces a transition to a (1×1) structure and still further heating to about 1050 K generates loss of long-range order in the surface region.[55] At 1211 K the crystal melts.

Since no quantitative structure analysis has been performed for the Ge(111)-(2×1) structure, evidence for its existence and detailed structural parameters arises from theoretical total energy calculations and the comparison of the associated excitation spectra with experimentally determined surface-state excitation spectra obtained from angle-resolved photomission spectroscopy (ARPES) for occupied surface states or inverse photoemission spectra (IPES) for unoccupied surface states. The first of these[100] predicted a π chain like that shown in Figure 7 and yielded a qualitative description of available ARPES data.[101] The second[102] found a slightly relaxed version of the same structure but achieved an improved description of both the occupied surface state excitation spectra obtained from ARPES data[101,103] and the unoccupied excitation spectra obtained from IPES.[104] The third[105] predicted two degenerate structures in which the top layer π chains were tilted much more and displaced sidewise to the right or to the left of the Pandey π chain structure. These also provide good descriptions of the ARPES data of Nicholls *et al.*[101,103a] Thus, these two structures join the three-bond-scission structures of Haneman and co-workers[37] as challenges to the Pandey π chain structure. It seems possible that they are not kinetically accessible from the cleavage face, but the resolution of this ambiguity awaits a quantitative structure analysis of the Ge(111)-(2×1) structure. As described for Si(111)-(2×1) in section V.A, these structures are compatible with the five principles of semiconductor surface reconstruction specified in section IV.

The stable low-temperature c(2×8) structure is shown in Figure 12. Summaries of its early history are given by Phaneuf and Webb[53a] and by Takeuchi, Selloni, and Tosatti.[106] Principle 1 is satisfied because the four adatoms per unit cell tie up all the substrate dangling bonds except those of the four remaining rest atoms. The associated orbitals form bonding surface states which are completely occupied,[107] leading to satisfaction of principle 2, although a complete theoretical description of their origin is not yet available. Charge is transferred from the adatoms to the rest atoms, leading to rehybridized filled lone pair orbitals on these atoms which are, however, almost certainly hybridized with orbitals from other atoms.[54,109] Since this structure

is the equilibrium low-temperature structure reached from a variety of surface processing conditions, principle 3 is also satisfied. Thus, the principles of semiconductor reconstruction are satisfied by both Ge(111)-(2×1) and Ge(111)-c(2×8).

Quantitative surface structure analyses of Ge(111)-c(2×8) have been performed using glancing-angle X-ray diffraction,[50] ion scattering,[110] LEED,[111] and X-ray crystal truncation rod analysis.[112] Surface images and their interpretations have been generated repeatedly by STM.[53b,54,108,113] The only complete theoretical structural prediction is that of Takeuchi, Selloni, and Tosatti.[106] The adatom nature of the structure shown in Figure 12 is well established, as are the general features of the atomic coordinates, although small differences between the various analyses remain. An informative comparison with the Si(111)-(7×7) structure has been given by Vanderbilt[52] who argues that the cost in energy of generating stacking faults and corner holes for Ge(111) is simply too high to to be compensated by dimer wall domain boundaries. Hence the patterned defect DAS structure which occurs on Si(111) does not occur on Ge(111). The result is a weakly bound, easily disordered c(2×8) adatom structure which coexists with regions of other local structures on Ge(111), as observed.

D. Ge(100)

The literature on Ge(100) is more sparse than that on Ge(111). Reviews of selected aspects have been given by Mönch[11] and by LaFemina.[12] The general pattern of the changes in structure with temperature is analogous to that[83] of Si(100): i.e., a low temperature c(4×2) phase reversibly becoming a (2×1) phase at about 200 K and subsequently exhibiting another order−disorder transition at 955 K before melting.[114] We begin our literature coverage in 1987, at which time the c(2×4) symmetry of the low-temperature ($T \leq 150$ K) structure had been established as described in a paper[115] on He diffraction in which pointers may be found to earlier LEED, ion scattering, and photoemission studies. In 1987 this paper, an earlier one on ion scattering,[116] and a contemporary one on glancing angle X-ray reflection,[117] constituted the only quantitative surface structure analyses for Ge(100)-c(2×4). All three supported dimer models, with He diffraction providing the most decisive confirmation of the tilted dimer atomic geometry shown in Figure 15. During 1987 a detailed STM study[118] of Ge(100) at room temperature revealed regions of (2×1), c(4×2), and p(2×2) analogous to the corresponding results for Si(100), but with fewer missing dimer defects. Analysis of the bias dependence of these images led to confirmation of the structure of these regions as being suitable configurations of tilted dimers. Thus, the Ge(100) surface structures seemed analogous to those observed for Si(100), and hence compatible with the principles of surface reconstruction as described in section V.B.

Subsequent experimental structure determinations confirmed the Si(100)−Ge(100) analogy at low and moderate temperatures ($T \leq 300$ K), while adding more detail to the description of the high-temperature order−disorder transition. Refinements to glancing-angle X-ray analysis permitted this technique to provide a detailed quantitative structure analysis[119] which confirmed the asymmetry of the dimers and provided structural coordinates of the top 10 atomic layers of the crystal. Moreover, the tilted dimers were imaged directly by high-resolution UHV transmission electron microscopy.[120] A second reversible phase transition at $T = 955 \pm 7$ K was discovered[121] by X-ray diffraction and suggested to be a surface roughening transition. A similar study[122] was made of the broad c(4×2)-(2×1) transition between 200 and 300 K with the result that the number of tilted dimers was conserved through this transition. Both phase transitions were then examined using high-resolution core level spectroscopy.[114] All of these results butressed the basic notion that tilted dimers are the fundamental structural motif in the low and medium temperature structures as expected from the first two principles of semiconductor surface reconstruction.

Theorists also have been active with respect to this surface. The first definitive prediction of the lower symmetry c(4×2) low-temperature Ge(100) structure was made by Needels, Payne, and Joannopoulos[32a,123] in 1987, although they were unable to distinguish its energy from that of the p(2×2) structure. Comparison with symmetric dimer structures was performed later by Spiess, Freeman, and Soukiassian[124] who noted that unlike Si(100), the asymmetric dimer on Ge(100) exhibits a significantly lower energy than its symmetric counterpart and hence would be more readily observed in STM images, as in fact had been found earlier.[118] An analysis[125] of the energetics and characteristics of the low-temperature order−disorder (200−300 K) phase transition on Ge(100) also has been given. Further, calculation of the excitation energies of the occupied surface state bands on Ge(100)-(2×1), based on prior theoretical studies of this system,[126] permitted a semiquantitative confirmation of the tilted dimer model,[127] although an observed dispersionless band of states was not described the the theory (a situation reminiscent of that for Ge(111)-(2×1)[101−103]). The most recent contribution is an analysis of the structural trends between the (2×1) dimer structures on the (100) surfaces of Ge, Si, and diamond.[86] Using LDF methods, Krüger and Pollmann[86] show that for Si and Ge the surface dimer π bond is sufficiently weak that the surface would be metallic without the Peierls distortion mandated by principle 2, which leads to the tilted dimer structures. On diamond, however, the C−C π bond is strong enough that the the surface is semiconducting even with a symmetric dimer geometry. Moreover the symmetric dimer is the lowest energy state for this material, with the symmetric and tilted dimers being nearly degenerate for Si(100) and the tilted dimer being clearly favored for Ge(100). Thus, these (100) surfaces illustrate clearly the interplay between principles 1 and 2. If the local chemical bonding is strong enough to generate saturated local surface bonds, principle 1 suffices to describe the surface bonding. If not, as is the case for both Si and Ge, then additional solid-state effects come into play as described by principle 2 to produce semiconducting surface state excitation spectra and the accompanying surface structural relaxations. Hence, both experimental results and total energy

calculations on the (100) surfaces of elemental tetrahedrally coordinated semiconductors reveal clearly the power and validity of the principles of semiconductor surface reconstruction articulated in section IV.

VI. Compound Semiconductors

As in the case of elemental semiconductors, the literature of the surface reconstructions of compound semiconductors is sufficiently vast (many hundreds of papers) that it is not useful to attempt a comprehensive treatment of it. Our strategy for dealing with this literature is to select one or more recent reviews as starting points and to provide discussions of the satisfaction of the principles of surface reconstruction and of recent results since those reviews. For the non-polar cleavage surfaces, this approach permits a consideration of all the materials studied to date because of the availability of two detailed recent reviews[5,7] covering the extensive prior literature. For the polar surfaces, however, the literature is equally extensive but much more fragmented. Although an excellent historical review[4a] and a comprehensive accounting[12] for theoretical calculations through 1991 have appeared recently, it seemed appropriate for our present purposes to select the most thoroughly examined polar surfaces, i.e., those of GaAs, to use as examples of the current state of the art. A more general account in monograph format has been given recently by Mönch.[11]

A. Zincblende Cleavage Faces

The non-polar (110) cleavage faces of zincblende structure binary compound semiconductors are the most extensively studied surfaces in semiconductor surface science.[4−7,9,11,12] Quantitative structure analyses and theoretical predictions are available for nearly all naturally occurring zincblende structure binary semiconductors (AlP, AlAs, GaP, GaAs, GaSb, InP, InAs, InSb, ZnS, ZnSe, ZnTe, and CdTe) as well as some like CuCl and CuBr which are grown in zincblende structure only by heteroepitaxy on lattice-matched substrates (GaP and GaAs, respectively). These studies are important because they reveal hitherto unsuspected scaling laws between the surface structures of different materials, thereby illuminating commonalities between III−V, II−VI, and I−VII compounds which cannot be interpreted in terms of local coordination chemistry considerations alone.[1,2,4,5,7,11,12] Thus, they were instrumental in motivating the proposal of the last two of the five principles of semiconductor surface reconstruction articulated in section IV. Since extensive recent reviews of this body of work are available,[5,7,11,12] we proceed by first indicating the operation of the five principles for these surfaces and subsequently noting additional work since these reviews.

The structure of the zincblende(110) cleavage faces is shown in Figure 4. For III−V semiconductors we can invoke principle 1 by noting that both the anions (e.g., As) and cations (e.g., Ga) form saturated valence conformations (s^2p^3 and sp^2, respectively) analogous to related small molecule geometries (e.g., AsH_3 and $Ga(CH_3)_3$). The surface is semiconducting, thereby satisfying principle 2, because of charge transfer from

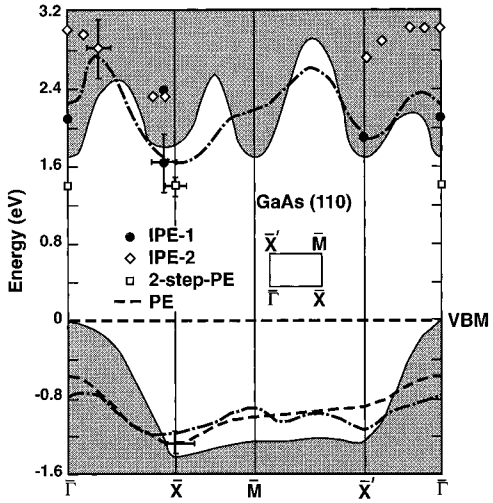

Figure 17. Filled (mostly As-derived) and empty (mostly Ga-derived) surface-state bands associated with the GaAs-(110) structure illustrated in Figure 4. The Brillouin zone associated with the surface unit cell is shown in the inset. The calculated excitation spectra are shown by heavy dot-dashed lines. The projection of the bulk bands is shown as the shaded area. The occupied surface states, obtained from photoemission experiments,[131] are shown by a dashed line indicated by PE in the figure. The unoccupied states obtained from two inverse photoemission experiments are designated by IPE-1[133] and IPE-2.[134] Prominent features in two-step photoemission are indicated by two-step PE.[132] These need not be asssociated with surface state excitations. (From Zhu *et al.*, ref 129a, with permission.)

the ($^3/_4$ occupied[25]) "dangling bond" of the cation to the ($^5/_4$ occupied[25]) "dangling bond" of the anion which then rehybridizes to become a completely occupied lone pair orbital, leading to the small-molecule geometries just noted. This rehybridization is allowed kinetically because there is no barrier to the rehybridization-induced relaxation,[35,38,67,128] thereby satisfying principle 3 as well. Principle 4 is satisfied because the $^3/_4$ of an electron in the cation dangling bond is simply transferred to the $^5/_4$ occupied anion dangling bond, yielding no net charge accumulation on the surface. Principle 5 is a restatement of principle 1 in terms of delocalized surface-state bands. The surface-state bands associated with the fully occupied anion "dangling bond" states of an unrelaxed surface rehybridize upon relaxation, lowering their energy and thereby driving the surface geometrical relaxation.[5,7,67] This principle is directly testable, moreover, by comparison of the predicted filled bands with ARPES data. *Ab initio* calculations of these filled surface state excitation energies recently have appeared in the literature.[129,130] We show the first of these[129] in Figure 17 in which they are compared with the results of single-step photoemission[131] (occupied states), two-step photoemission[132] (mixed), and inverse photoemission[133,134] (unoccupied states) measurements. The correspondence between the calculated and measured occupied surface state bands is excellent, although the situation for the unoccupied states is more complicated.[129] Figure 17 reveals clearly that the delocalized surface-state band representation of the relaxation-induced surface charge density provides a quantitative explanation not only of the surface atomic geometry, but also of the surface state excitation spectra as measured directly by photoemission experiments. Hence, it

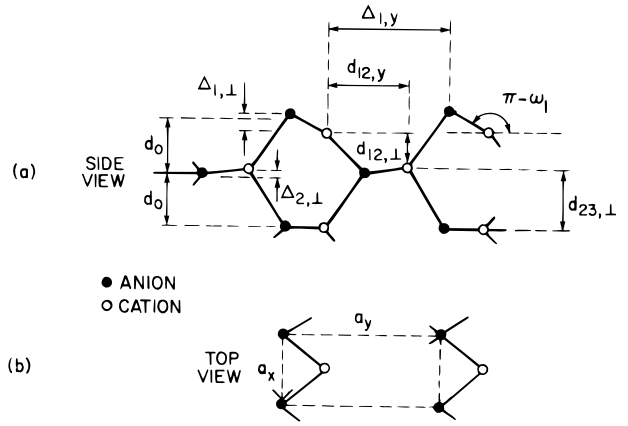

Figure 18. Panel a: Schematic indication of the surface atomic geometry of the (110) cleavage surface of zincblende structure compound semiconductors. The layer spacing is $d_o = a_o/2\sqrt{2}$ in which a_o is the bulk lattice constant. The top layer tilt angle, labeled ω_1 in the figure, is designated by ω in the text. Panel b: Surface unit cell. Surface unit mesh parameters are $a_y = a_o$ and $a_x = a_o/\sqrt{2}$. (From Duke, ref 7, with permission.)

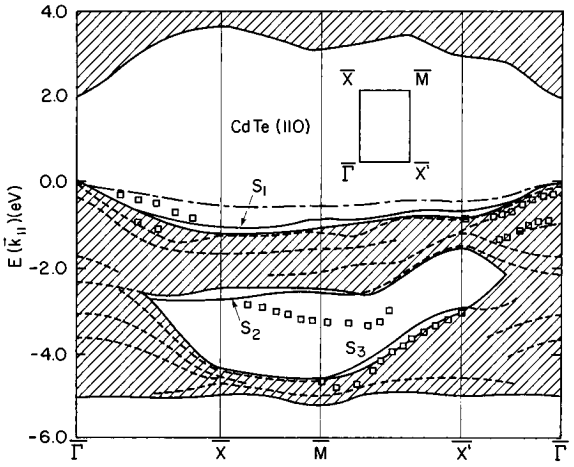

Figure 19. Surface state-energies for the (110) surface of CdTe. The surface Brillouin zone is indicated in the inset. The squares designate the experimentally determined surface-state energies. The surface states and resonances calculated using a tight binging total energy model are shown by solid and dashed lines, respectively. The shaded areas indicate the projection of the bulk band structure on the surface excitation spectra. The dot-dashed line designates the Te dangling bond surface states (S_1) characteristic of the unrelaxed CdTe(110) surface. (After Wang *et al.*, ref 138, with permission.)

affords a suitable generalization of the local coordination chemistry model (as embedded, e.g., in principle 1] to extend to II−VI and I−VII compound semiconductors.

One clue that the (110) cleavage faces might exhibit unusual structural features across the III−V, II−VI, and I−VII materials is the invariance of the electron-counting-rule[25,56] predictions (i.e., principle 4) on the nature of the surface anions and cations. For both II−VI (anion dangling bonds containing $^3/_2$ electron and cations $^1/_2$ electron) and I−VII (anon dangling bonds containing $^7/_4$ electron and cation $^1/_4$ electron) one obtains the same result as for the III−V compounds that at the surface the fractional charge in the cation dangling bond is transferred to the anion to generate a completely full band of (primarily) anion-derived surface states. This result contrasts sharply with those for the polar surfaces, for which the counting rules predict markedly different structures for the three classes of compounds.[25,45,46,48,56−58] It is, however, compatible with the remarkable and unexpected result, discovered in 1983,[62] that to within experimental uncertainties at that time all zincblende (110) surface structures are identical when measured in units of the bulk lattice constant and correspond to a bond-length-conserving rotation of the top atomic layer leading to tilt angles, indicated schematically in Figure 18, of 29° ± 3°. Full accounts of this discovery and its subsequent confirmations and extensions to wurtzite structure cleavage faces may be found in the reviews cited.[4,6,7,12] Although it is currently (1993−5) being recognized that with improved structure analysis techniques extensions to this result to include the effects of ionicity on the most ionic II−VI and I−VII can be achieved,[135−137] the results of the early studies have been repeatedly validated by subsequent work,[4,5,7] revealing a scaling rule which is unanticipated by the local coordination chemistry of the II−VI and I−VII materials.

Principle 5 is our response to this situation. It describes all known results on the zincblende and wurtzite cleavage faces[7] and is believed to describe those on the polar surfaces as well.[12] This principle replaces the local charge densities as the carrier of coordination chemistry information with the extended surface state energy bands characteristic of 2D surface compounds. These have the added advantage that they are directly accessible to experimental determination via, e.g., ARPES. Having noted the testability of this point of view for GaAs(110) in Figure 17, we show comparable results[138] for CdTe(110) in Figure 19. While the calculation for CdTe is based on a phenomenological tight-binding total energy model (with parameters selected to predict bulk optical and electrical properties), this model has predicted quantitatively the geometries and dangling-bond bands of other III−V and II−VI compounds.[67] It also predicts the major features of the measured surface state spectra, although its shortfalls become increasingly evident for the deeper states labeled by S_2 and S_3. *Ab initio* LDA methods also have been applied to the II−VI compounds,[136,137,139] but their level of maturity has not yet reached that of the group IV and III−V compounds as reflected, e.g., in Figures 13, 16, and 17. It is evident from Figure 19 that the Te-derived dangling-bond surface states, labeled by S_1, have been lowered in energy by the surface relaxation and thereby stabilized this relaxation as predicted by principle 5. Since the tight-binding total energy model also gives a quantitative prediction of the observed structure of CdTe(110),[67b,138] this example reveals the power of principle 5 to predict results which are not accessible to models based solely on local coordination chemistry.

Additional work since the recent reviews of Kahn,[4a] Duke,[5,7] and LaFemina[12] has been focused on applying new techniques to determine the surface geometrical and electronic structure of (110) cleavage faces, especially GaAs and InP. For GaAs(110) new structure analyses have been reported on the basis of positron diffraction,[140,141] STM,[142] and photoelectron diffraction.[143] For InP(110) they have been reported using positron diffraction,[140] STM,[144] X-ray

standing waves,[145] EXAFS,[146] and photoelectron diffraction.[147] The main revelation of these analyses is the pressing need for quantitative error (uncertainty) analyses in the estimation of the values of the parameters describing the details (e.g., tilt angles to within a few degrees, bond length changes by 0.1 Å or less) of surface structures. They all report structures in general agreement with those given earlier but differing among themselves on the small changes in detail, or lack thereof, from prior analyses. In each case a "best fit" to some data set is obtained (or a particular theoretical model is tested) and uncertainties in the structural parameters may or may not be estimated, with minimal concern for sampling errors inherent in the selection of the data sample, systematic errors incurred by virtue of the model used to analyze this sample, and the adequacy of the best fit criterion to yield a statistically significant analysis of the uncertainties inherent in the estimation of the structural parameters. Thus, it is hardly surprising that the various methods often generate structures outside each others putative error bounds and hence provide structural parameter estimates of questionable utility for the refinement of the surface structures reported earlier.[4,5,7,9,11] This is an inevitable difficulty that a field has to face when it develops to the point of having multiple techniques purporting to provide quantitative estimates of structural variables. Studies of the detailed atomic geometries of the (defect free) zincblende (110) surfaces have reached this point during the past few years, so further progress on refining these geometries and identifying chemical trends, e.g., with ionicity of the substrate, depends upon the formulation and adoption of greatly improved error analyses.

B. Wurtzite Cleavage Faces

Many II−VI compounds crystallize in the wurtzite crystal structure, e.g., ZnO, ZnS, CdS, and CdSe. These materials exhibit two nonpolar cleavage faces, the $(11\bar{2}0)$ surface illustrated in Figure 6 and the $(10\bar{1}0)$ surface shown in Figure 9. The $(11\bar{2}0)$ surface exhibits a chain motif, analogous to zincblende(110), but contains four rather than two atoms per unit cell, although both anions and both canions are symmetry equivalent due to a glide plane symmetry. A detailed discussion of the structure and symmetry of this surface is given by Kahn *et al.*[148] The $(10\bar{1}0)$ surface, on the other hand, exhibits a dimer motif as is evident from Figure 9. A discussion of the structure and symmetry of this surface is may be found in Duke *et al.*[149] During the past three years thorough reviews of the theoretical prediction and experimental determination of the structures of both surfaces have been given[5,7] to which the reader is referred for a discussion of these topics.

The application of the principles of semiconductor surface reconstruction to these surfaces mirrors their application to zincblende(110) surfaces as described in the preceding section. Both surfaces are autocompensated because they contain equal numbers of anions and cations, thereby satisfying principle 4. They are semiconducting, satisfying principle 2, because the $^1/_2$-occupied cation dangling bond electrons are transferred to the $^3/_2$ occupied anion dangling bond states creating a filled occupied surface

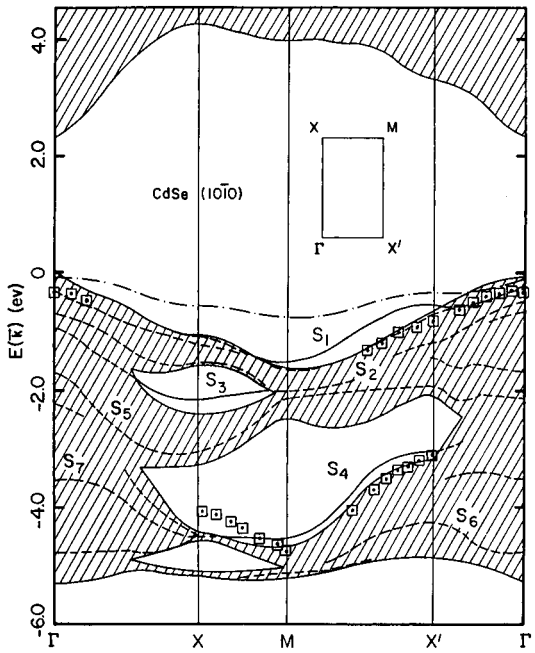

Figure 20. Surface state energies for the $(10\bar{1}0)$ surface of CdSe. The surface Brillouin zone is indicated in the inset. The squares designate the experimentally determined surface-state energies. The surface states and resonances calculated using a tight binging total energy model are shown by solid and dashed lines, respectively. The shaded areas indicate the projection of the bulk band structure on the surface excitation spectra. The dot-dashed line designates the Se dangling bond surface states (S_1) characteristic of the unrelaxed CdSe$(10\bar{1}0)$ surface. (After Wang *et al.*, ref 150, with permission.)

state band of anion-derived surface states. This band then rehybridizes, causing a relaxation of the surface species and lowering the energies of these surface states in keeping with principle 5, until the anion achieves a roughly s^2p^3 local conformation and the cation a sp^2 conformation.[68] These rehybridizations are kinetically accessible, in accordance with principle 3, because no barrier exists for these (approximately bond-length-conserving) rotational relaxations.[68] As noted in the preceding section, for these compound semiconductors principle 5 is the operative restatement of principle 1, so the cleavage surfaces of wurtzite as well as zincblende structure compound semiconductors satisfy the principles of semiconductor reconstruction articulated in section IV.

Building on our discussion of the zincblende(110) surfaces, we note that the consequences of principle 5 are directly observable by ARPES. For the wurtzite structure surfaces, this expectation has been validated explicitly in only two cases, CdSe$(10\bar{1}0)$[150] and CdS$(10\bar{1}0)$.[151] We show in Figure 20 a comparison between the calculated and observed surface state energies for CdSe$(10\bar{1}0)$.[150] It is evident from the figure that the relaxation of the surface has greatly lowered the energies of the Se-derived S_1 band of surface states and that the resulting predictions of the surface state energies of the relaxed surface are in excellent correspondence with the observations. The model used in these calculations is a phenomenological tight-bonding model like that used to obtain the model predictions shown in Figure 19, so similar caveats to those given in the preceding section apply to its prediction of the deeper lying surface

state energies. Nevertheless, Figure 20 reveals another experimental verification of the notion that the delocalized surface states are the carriers of the the surface chemical bonding for the cleavage faces of the III−V, II−VI, and I−VII tetrahedrally coordinated compound semiconductors. Moreover, both the model predictions and the experimentally determined structures of the wurtzite as well as zincblende cleavage surfaces reveal the description of the systematics observed over the entire range of structures and materials by the five principles of semiconductor surface reconstruction.

The major additional results on these surfaces since the recent reviews[5,7,12] are *ab initio* analyses[151−153] of the $(10\bar{1}0)$ surfaces of ZnO and CdS and application of both LEED and low-energy positron diffraction (LEPD) to determine the structure of the $(10\bar{1}0)$ and $(11\bar{2}0)$ surfaces of CdSe.[154] The *ab initio* analyses largely confirm the results of prior tight-binding calculations,[155,156] but give slightly different structures[151,152] for ZnO$(10\bar{1}0)$ which are equally compatible with available experimental measurements. Comparison of the structural parameters for CdSe$(10\bar{1}0)$ emanating from LEED and LEPD reveals that their compatibility lies at the extremities of the error estimates of the two methodologies, although both validate the theoretical predictions[150] of these parameters to within experimental uncertainty. Better descriptions of the experimental intensity data are obtained for LEPD than for LEED, as is the case for the (110) surfaces of GaAs and InP, as well.[140] This result seems to emanate for the fact that the model of the diffraction process is more accurate for LEPD than for LEED due to the nature of the positron−solid versus electron−solid interaction.[157] The small, but apparently systematic, discrepancies between the structural parameters extracted from the two analyses for binary semiconductors with anions and cations from different rows of the periodic table further butresses the importance of establishing thorough error analysis procedures, as indicated in the previous section for the zincblende-(110) surfaces.

C. GaAs(111) and $(\bar{1}\bar{1}\bar{1})$

Two fine discussions of the evolution of structural studies of the (111) and $(\bar{1}\bar{1}\bar{1})$ polar surfaces of zincblende structure materials have recently appeared,[4a,11] although they do not cover completely the theoretical literature. This literature prior to 1992 is reviewed, however, by LaFemina.[12] Thus, we confine our attention in this section to a consideration how the principles of semiconductor surface reconstruction articulated in section IV apply to these surfaces and to an indication of the recent developments since 1991 which lie outside the scope or time period covered by these reviews. We further restrict our systematic literature coverage to GaAs, since by far the most material is available for this semiconductor.

The primary structure observed[4,11,40] on the Ga-terminated GaAs(111) surface (often referred to as the (111)A surface in the literature) is the (2×2) Ga vacancy structure indicated in Figure 5. As noted in section III, this structure has been observed for GaP,[41] GaSb,[42] and InSb[43] as well. The structures of all polar surfaces depend, however, upon the preparation conditions for the surface. A good indication of the resulting complexities for the Ga terminated (111) surface may be found in Thornton *et al.*[158] and for the As terminated $(\bar{1}\bar{1}\bar{1})$ (often referred to as the (111)B surface) in Ranke and Jacobi.[159] A useful description of how this circumstance is handled in the calculation of free energies for the various surface structures is given by Kaxiras *et al.*[160] The importance of principle 3 (kinetic accessibility) in interpreting structural data has recently been reemphasized, however, by a report[158] that multiple structures are associated with the (2×2) LEED pattern on GaAs(111) depending upon the preparation conditions. Multiple local minima occur in the free energy.[160,161] Which one is obtained in a given experiment is determined by principle 3.

The cation vacancy structure indicated in Figure 5 satisfies the last two principles of semiconductor surface reconstruction for all III−V, II−VI, and I−VII materials. Since there are four cations per unit cell without the vacancy, three are left when it is generated. Yet generation of the vacancy generates three anion dangling bonds in the second layer, which exactly compensate the remaining three cation dangling bonds. Stated alternatively, the generation of a cation vacancy renders the (111) surface effectively nonpolar just like the (110) surface. Independent of the occupancy of the dangling bond states ($^5/_4$, $^3/_2$, and $^7/_4$ for anions and $^3/_4$, $^1/_2$, and $^1/_4$ for cations on III−V, II−VI, and I−VII compounds, respectively) charge transfer from the cations to the anions generates a completely occupied anion-derived nonbonding lone pair surface state band whose rehybridization induced lowering in energy can stabilize the surface. Such a relaxation does occur, with the remaining Ga species in the top layer sinking to become almost coplanar with the As in the layer beneath. A quantitative structure analysis of this surface by LEED has been given by Tong *et al.*[40a] The GaAs-(111)-(2×2) surface becomes electronically almost equivalent to the GaAs(110) surface in that 12-membered rings, which exhibit the nearest neighbor (110) chain structure except for the fact that three As species in each ring (one As per unit cell) are 4-fold rather than 3-fold coordinated, cover the surface. Thus, principles 2, 4, and 5 are satisfied. Since for compound semiconductors, principle 1 is superseded by principle 5 and principle 2 is encompassed by principle 4, we use only principles 3−5 in our considerations in this and subsequent sections.

Only principle 3, kinetic accessibility, remains. The cation vacancy structures are made by a variety of means: ion-bombardment and annealing a precut crystal, direct generation by MBE, and generation by capping MBE grown crystals and then uncapping them in UHV. Empirically most of the methods seem to generate the cation vacancy structure, although decapping in a fashion which generates an excess of As is reported to lead to an As trimer structure.[158] Since the same structure is generated by a variety of processes and process conditions, it represents a minimum in the free energy, as calculated theoretically.[39,160,161] Therefore subject to kinetic accessibility, we expect cation vacancy structures to occur on the (111) surfaces of III−V, II−VI, and I−VII

zincblende structure compound semiconductors. Indeed, they have been reported to be even more stable on ZnSe than on GaAs.[162]

Unlike the situation for GaAs(111), for GaAs($\bar{1}\bar{1}\bar{1}$) a variety of different symmetry structures commonly occur depending upon the processing conditions.[4,11,159] The (2×2) structure which occurs for this surface is generally believed to be the As trimer structure illustrated in Figure 10.[48,163] All of the evidence for this structure on GaAs is obtained by STM.[48,163] No quantitative structure analysis is available for GaAs, although one for InSb($\bar{1}\bar{1}\bar{1}$)-(2×2) via transmission electron microscopy has been given recently[164] which confirms an Sb trimer structure. Other structures also have been observed,[4,11,159] including ($\sqrt{3}\times\sqrt{3}$), (3×3) and ($\sqrt{19}\times\sqrt{19}$). Considerable theoretical effort has been devoted to the ($\sqrt{19}\times\sqrt{19}$) structure,[25,160b] but thus far no fully satisfactory proposed structure has emerged.

The As trimer structure also satisfies the principles of semiconductor reconstruction. Each As in the trimer contributes $^3/_4$ of an electron to complete the bond to the As in the substrate beneath. Four As species occur in the substrate unit cell, however, so an additional $^3/_4$ electron must be contributed from the trimer to complete the extra As dangling bond orbital. The remaining 12 electrons in the As trimer are used to bond the As to each other (6 electrons) and to complete the As lone pair orbitals of the trimer (6 electrons). Hence, principles 4 and 5 are satisfied simultaneously. The trimer is stabilized relative to adatom geometries (which also satisfy the autocompensation rule) because the bonds are much less strained.[160] The fact that all of the As lone pair orbitals are filled gives a semiconducting surface, so principle 2 is satisfied automatically, as noted earlier. Principle 3 indicates that this structure must be accessible in an As-rich environment, since the trimer is predicted to by the minimum free-energy structure in such an environment.[48,160,161] This is the case experimentally.[48]

Recent experimental work includes the discovery of an As trimer GaAs(111)-(2×2) structure[158] and an extension[163] of the work on Pashley and co-workers[26] on GaAs(100) to show that defects on the GaAs($\bar{1}\bar{1}\bar{1}$)-c(2×2) surface accumulate enough charge to exactly compensate the space charge. This is significant as an independent confirmation of the validity of principle 4: charge neutrality at the surface which becomes autocompensation at the surface in the absence of space charge. A careful and useful comparison and extension of previous[48,160] LDF studies of the various proposed (111) and ($\bar{1}\bar{1}\bar{1}$) structures was published,[161] revealing agreement on the points described above for the vacancy and trimer structures at Ga excess and As excess extremes, respectively, but significant differences between the two models' predictions elsewhere in the surface phase diagram. Finally, a cluster calculation of surface structures was given[165] which contains an extensive account of earlier literature on the GaAs(111) and ($\bar{1}\bar{1}\bar{1}$) surfaces.

D. GaAs(100)

GaAs(100) forms a variety of structures as a function of processing conditions and surface stoichiometry. As evident from the numerous STM micrographs of this surface, dimers are the primary motif. If we adopt the convention, implied by Figure 8, that As dimers form along the vertical axis, then in order of decreasing [As]/[Ga] ratio a series of structures is formed in the order[45] c(4×4), c(2×8), 1×6, 4×6, and c(8×2). Moreover, the c(2×8) [(8×2)] structures are built out of (2×4) [(4×2]] units, such as that shown in Figure 8, and there are at least four serious candidates[60] for the structure of the As dimer (2×4) units, designated by α, β, γ, and α_{sym}. The history[11] of studies of these surfaces is replete with complex diagrams describing the process dependence of the various symmetry structures and descriptions of the difficulties in establishing surface compositions for each. Even today (mid-1995) the structures of these surfaces are the subjects of intense interest and controversy.[59,166,167] Thus, our approach to these surfaces is to use them as an example of how to apply the principles of semiconductor surface reconstruction prospectively rather than retrospectively. That is, we will use them to propose prospective structures and to evaluate experimental and theoretical information as they became available. A fairly complete account of the pre-1993 literature has been given by Mönch,[11] which we take as the starting point of our discussion.

Analysis of a new structure may be visualized to proceed in six schematic steps. First, a range of experimental process conditions is established which give a reproducible stable structure of a given symmetry. Second, a surface motif for this structure is postulated either from experience or from experimental suggestions like STM micrographs. Third, principles 4 and 5 are applied simultaneously to generate a sample of possible structures which are both electrically (principle 4) and chemically (principle 5) reasonable. Then detailed structural models are constructed either from chemically sensible bond lengths and angles (using, e.g., sums of covalent radii for bond lengths and geometries of analogous structures for local bonding conformations) or via a free-energy minimization calculation to obtain the structural coordinates of a local equilibrium structure. Fifth, the proposed structural models are refined by comparison of the predictions of experimental measurements by the structural model. Typically diffraction spectroscopies like LEED, RHEED, LEPD, EXAFS, photoemission diffraction, or transmission electron diffraction from a thinned sample are required to generate the detailed atomic coordinates of the surface species. Photoemission measurements of the occupied surface state bands and inverse photoemission or optical absorption measurements of the empty surface state bands are helpful at this stage for qualitative confirmation of a structure, but cannot usefully be inverted to generate atomic coordinates. Finally, steps four and five are iterated until a theoretically sensible (e.g., minimum free energy) structure is found which is quantitatively compatible with all the available experimental data and can be rationalized as resulting from the associated process conditions in terms of principle 3. The major role of the principles of semiconductor surface reconstruction in this process is to reduce the number of candidate structures to a manageable number [e.g.,

three to five in the case of a particular stoichiometry of GaAs(100)] which are chemically, electrically and kinetically plausible. Only detailed analysis of experimental structure-sensitive data suffices to determine the actual atomic coordinates which define the surface structure.

We next apply this process to the c(2×8) structure on GaAs(100) for which the initially proposed structure[45] is shown in Figure 8. The experimental preparation of this structure by molecular beam epitaxy (MBE) in several different laboratories had been established by the late 1980s.[11,45,46] STM micrographs revealed that dimers were the primary surface motif and that missing dimers occurred in this structure.[45,46] Envisage these dimers to be comprised of As atoms on a Ga-terminated ideal (100) substrate.[168,169] Then from principle 4 each dimer has 10 available electrons from the As species. But to satisfy principle 5, each dimer must have two electrons in the As−As bond, four electrons in the filled As-derived occupied surface-state bands, and 4 × ($^5/_4$) = 5 electrons to complete its four bonds with the substrate. Thus, each dimer is short one electron to fulfill principle 5, so we must propose a structure with some Ga dangling bond donor states to generate the needed extra electrons for the As dimers. For each missing dimer, there are four unsatisfied Ga dangling bonds each containing $^3/_4$ electron for a total of three electrons. Thus, each missing As dimer will generate enough electrons to satisfy the requirements of three As dimers. We are immediately led, therefore, to the three-surface-dimer model[168,169] shown in Figure 8, to which we refer as the $\beta(2\times4)$ structure.[60,169]

Other structures which satisfy principles 4 and 5 also can be readily constructed, as indicated in Figure 21 in which the $\beta(2\times4)$ structure is shown in panel a. If a row of Ga atoms is removed at the edge of two As dimers, the third dimer will occur on the third layer beneath the As surface species as shown in panel b of Figure 21. Evidently, this model, referred to as the $\beta2(2\times4)$ structure,[60] also satisfies principles 4 and 5 but with a lower value of [As]/[Ga] than the $\beta(2\times4)$ structure. Alternatively, we could inquire into the situations which arise with Ga dimers on the surface. Each Ga dimer has six electrons at its disposal. Two of these are required for the Ga−Ga bond and 4 × ($^3/_4$) = 3 are required for its four back-bonds to an As substrate. Thus, each Ga dimer has one extra electron to donate to an As dimer. Inspection of the geometry of the surface shows that the Ga dimers occur at right angles to the As dimers, so an obvious structure is one in which a pair of As dimers is accompanied by a pair of Ga dimers as shown in panel c of Figure 21. This geometrical model, called the $\alpha(2\times4)$ structure[60,169] exhibits a still lower value of [As]/[Ga] than the $\beta2(2\times4)$ structure. If the As dimers lie at the ends of the unit cell and the Ga dimers in the center the structure is referred to as the $\alpha_{sym}(2\times4)$ structure.[60] Another class of termination models which give larger values of [As]/[Ga] than the $\beta(2\times4)$ structure may be constructed by using an As terminated surface as the substrate for As dimers. In this case, each dimer needs only 4 × ($^3/_4$) = 3 electrons in its back-bonds (because the substrate As species contribute $^5/_4$ electron to each bond) so a total of nine electrons is required per dimer, whereas 10 are available, i.e., As dimers on As substrates are donors rather than acceptors. This fact is exploited in constructing the extra dimer structure shown in panel d of Figure 21. The added dimer on top of the four As species donates the extra electron needed by the dimer on the Ga substrate beside it. Moreover, the four Ga dangling bonds associated with the missing As row each donate the $^3/_4$ electron just needed to fill the lone pair orbitals of the four 3-fold coordinated As species to which the added dimer is bonded. This model is referred to as the $\gamma(2\times4)$ structure[60,169] as indicated in the figure. An even more As-rich dimer structural model may be constructed by noting that since a missing row of As dimers on an As substrate generates 4 × ($^3/_4$) = 3 empty As dangling bond orbitals to be filled according to principle 5, a model consisting of three As dimers on an As substrate, as shown in panel e of Figure 21, satisfies principles 4 and 5. A block of four of these structures is believed to comprise the As-rich c(4×4) structure[45b] as indicated in panel e. Additional models for Ga rich surfaces can be constructed to be compatible with principles 4 and 5, e.g., Ga dimers on an As substrate[45b] or Ga trimers on an As substrate with dimerized As along missing Ga

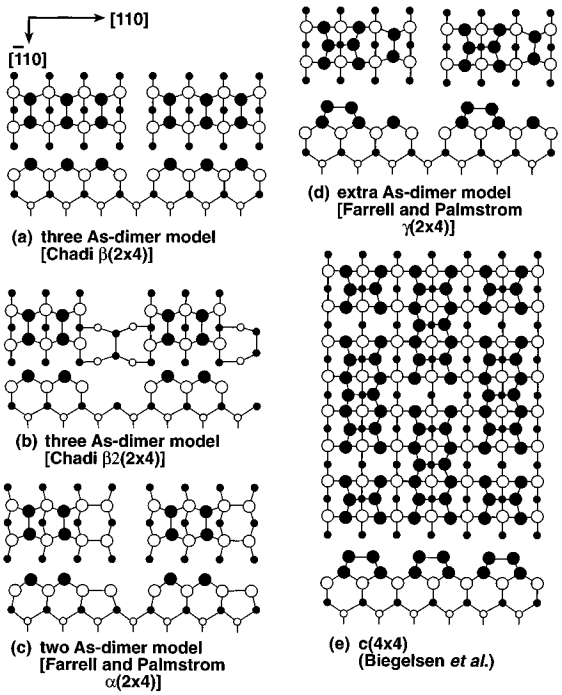

Figure 21. Schematic diagrams of proposed atomic geometries for the (2×4) As-rich structure on GaAs(100) and of the assembly of one of these models to form the c(4x4) structure. Panel a: Three top-layer As dimer model proposed by Chadi.[168] Designation as the $\beta(2\times4)$ structure is taken from Northrup and Froyen.[60] Panel b: Three As dimer (two in the top layer and one in the third layer) model proposed by Chadi.[168] Designation as the $\beta(2\times4)$ structure is taken from Northrup and Froyen.[60] Panel c: Two top-layer As, two second layer Ga dimer model proposed by Farrell and Palmstrøm.[169a] Designation as the $\alpha(2\times4)$ structure is taken from Northrup and Froyen.[60] Panel d: Extra As dimer model proposed by Farrell and Palmstrøm.[169a] Designation as the $\gamma(2\times4)$ structure is taken from Northrup and Froyen.[60] Panel e: Three top layer As dimer on As substrate structure of the c(4×4) structure as proposed by Biegelsen *et al.*[45b] (Adapted from Hashizume *et al.*, ref 166, with permission.)

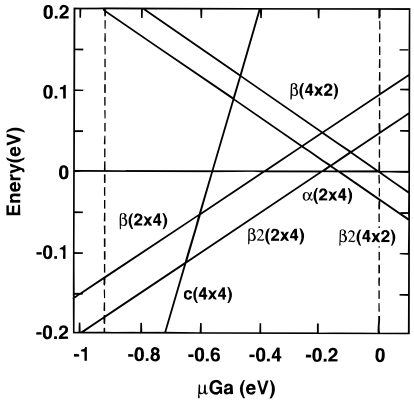

Figure 22. Formation energies per unit cell of selected surface structures on GaAs(100). The (2×4) structures for which results are shown in the figure are As-rich geometries indicated in Figure 21. The corresponding (4×2) structures are Ga-rich geometries in which the As and Ga species have been interchanged relative to Figure 21. Specification of each of the geometrical models may be found in Northrup and Froyen.[60] Vertical dashed lines indicate the allowed range of values of the chemical potential for Ga. (Adapted from Northrup and Froyen, ref 60b, with permission.)

rows.[59] Figure 21 shows, however, the array of candidate structural models which has been most extensively studied for the As-rich GaAs (100)-(4×4) and (2×4) structures.

Having enumerated a substantial list of candidate structural motifs, the next step in structure determination is to convert these motifs into detailed structural models to be tested by comparison with structure-sensitive measurements. For GaAs(100)-(2×4) this has been done largely through total energy calculations, starting with the pioneering work of Chadi in 1987,[168] who, using an empirical tight binding total energy model, found the $\beta(2\times4)$ and the $\beta2(2\times4)$ states nearly degenerate in energy. This work was followed shortly with a LDF analysis by Qian, Martin, and Chadi[170] who validated the energy lowering associated with the $\beta(2\times4)$ structure. Subsequently, in 1993, two LDF calculations were reported by Ohno[171] and by Northrup and Froyen[60] which led to differing structural predictions. Ohno emphasizes the important role of large surface relaxations from idealized starting geometries which stabilized the motifs shown in Figure 21, a result with which we are familiar from our discussion of the GaAs(111)-(2×2) structure in the previous section. A complication with which all of the calculations must contend is the specification of the ground-state free energy as a function of the composition of the surface. A useful discussion of this topic may be found in Qian *et al.*[170a] It is resolved by using the Gibbs free energy which is expressed as a function of the chemical potential of the reacting species, Ga and As. Since their sum must equal the formation energy per unit cell of bulk GaAs, however, only one chemical potential is an independent variable. Thus, results of LDF calculation are presented as plots of the Gibbs free energies for the various structural models as a function of one of the chemical potentials, as shown in Figure 22 for GaAs(100).[60b] In Figure 22 the chemical potential of Ga is taken to be the independent variable. Movement from left to right in the diagram corresponds to decreasing surface As concentrations, i.e., decreasing [As]/[Ga]. It is evident from the figure that the c(4×4) geometry shown in panel e of Figure 21 is the stable structure for high surface As concentrations, whereas the Ga-rich c(8×2) structure, comprised of Ga $\beta2(4\times2)$ dimer structures as shown in Figure 23, is the stable structure at high surface Ga concentrations. At values of [As]/[Ga] intermediate between these limits the $\beta2(2\times4)$ (panel b, Figure 21) and $\alpha(2\times4)$ (panel c, Figure 21), respectively are stable for decreasing values of [As]/[Ga]. Thus, these LDF calculations have not only specified detailed atomic geometries for comparison with experiment but also have established expectations for the lowest energy (i.e., most stable) surface structures at each surface composition.

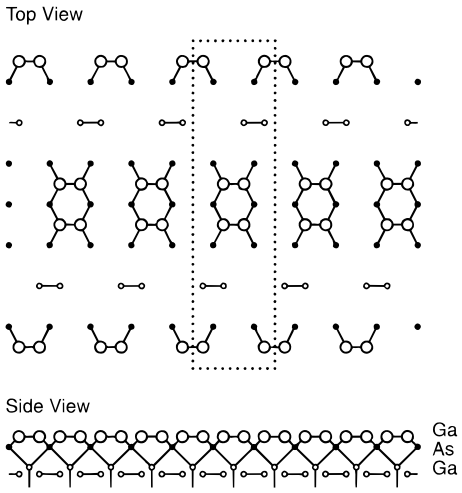

Figure 23. Schematic illustration of the GaAs(100)-c(8×2) [or (4×2)] reconstruction. Dashed lines indicate the surface unit cell. (Adapted from Biegelsen *et al.*, ref 45b, with permission.)

The experimental situation is complicated not only by the variety of surface compositions which are readily accessible by MBE, but also by principle 3, kinetic accessibility. Many of the achieved surface compositions and structures are metastable, analogous to the low temperature (2×1) cleavage structures of Si(111) and Ge(111), but less well defined. One of the early controversies when only STM micrographs were available concerned whether three ($\beta(2\times4)$, the "six pack") or two ($\beta2(2\times4)$ or $\alpha(2\times4)$, the "four pack") dimers were imaged in the c(2×8) structure. Early results[45] indicated the "six pack" whereas in time the majority of experiments[46, 166,172] favored the "four pack" as expected from the LDF results shown in Figure 22. Evidently, the $\beta(2\times4)$ structure is accessible kinetically, even though its free energy is higher than that of the $\beta2(2\times4)$.

The correspondence between specific atomic geometries and *in situ* RHEED patterns (which determine the $(n\times m)$ labels for the structures) has only partially been clarified over time. In 1990 Farrell and Palmstrøm suggested that the α, β, and γ motifs indicated in Figure 21 were associated with specific RHEED intensity fingerprints. Subsequent combined RHEED/STM experiments[166] revealed that all three RHEED patterns were associated with "four pack" atomic geometries, and that the experimental RHEED signatures were characteristic of much more complex surface atomic structures than a uniform coverage of one of the motifs shown in Figure 21. Similar

experiments[167] further resolved a controversy which had arisen[173] over the Ga-rich c(8×2) structure, confirming that it consisted of $\beta 2(4\times2)$ units as predicted by Figure 22. A proposal[174] that ordered surfaces characterized by good LEED patterns are associated with dimers which contain both Ga and As species was shown to be at variance with both total energy calculations[60] and STM data,[175] although the associated experimental ion scattering measurements have been claimed to be compatible with the As dimer "four pack" results of Hashizume *et al.*[166]

Few quantitative structure analyses have been reported. A glancing-angle X-ray analysis[176] of a c(4×4) structure did not yield satisfactory results for the c(4×4) motif indicated in Figure 21 leading the authors to conclude that the surface contained a mixture of the c(4×4) three top layer As dimer motif and a two As dimer on As substrate motif (which does not satisfy principle 4), for both of which the atomic coordinates of the top two layer As species were given. This model is at variance with available STM micrographs. Two more recent quantitative analyses of the (2×4) As-rich structures, one based on shadow-cone-enhanced secondary ion mass spectrometry[177] and another on X-ray photoelectron diffraction[47] are both based on the $\beta(2\times4)$ structural motif (panel a, Figure 21) which is now recognized not to be the dominant structure. Hence the quantitative validity of these results is uncertain, although qualitative features like the lack of dimer tilting are likely correct. Finally, a quantitative LEED intensity analysis has recently been published[178] for a Ga-rich c(8×2) structure prepared, however, by ion bombardment and annealing rather than MBE. This analysis favors the Ga analog of the six pack structure shown in panel a of Figure 21, i.e., the $\beta(4\times2)$ structure, as opposed to the $\beta 2(4\times2)$ structure shown in Figure 23 which is expected for the MBE grown material.[45b,60,167] Perhaps the ion-bombard anneal treatment kinetically accesses the less stable $\beta(4\times2)$ structure rather than the ground-state $\beta 2(4\times2)$ structure, thereby achieving compatibility between the total energy predictions shown in Figure 22 and the structure determined by LEED intensity analysis. This result is suggested by the fact that similar treatments for InSb(100) yield a $\beta(4\times2)$ six pack In dimer structure as determined by STM.[179] Examining this overall situation, it seems fair to conclude that at the present time (summer, 1995) there are no fully tested and confirmed quantitative structure determinations for any structure on GaAs(100).

Returning to our theme of using GaAs(100) as an example of prospective rather than retrospective structure analysis, we see that steps 1−4 indicated above have been completed. A number of structural motifs have been identified (Figure 21), confirmed by STM micrographs, and a few of them validated as equilibrium structures (Figure 22). Quantitative comparison of the atomic coordinates with structure sensitive measurements is, however, in its infancy, with available results still occasionally in apparent conflict. Thus, steps 5 and 6 are work in process. We have a good notion of what the structures ought to be, but significantly less information on what they actually are.

VII. Synopsis

Our objective in this article has been to present a coherent description of the surface atomic geometries of the low-index faces of tetrahedrally coordinated semiconductors in terms of five principles (in practice only three each for elemental and compound semiconductors) which govern the formation and properties of these structures. These principles, articulated in section IV, were shown in sections V and VI to describe the structures of all of the most highly studied low index faces of elemental and compound semiconductors, respectively. An important feature of these principles is their explicit incorporation of notions like surface state bands, Fermi surface instabilities, and kinetic accessibility which transcend the concept of local coordination chemistry. These additional concepts were shown to be required to give a coherent and comprehensive description of the semiconductor surface structures. Thus, these structures are appropriately visualized as new 2D compounds, epitaxically bonded to their bulk substrate, which exhibit properties distinct from either the corresponding bulk solids or molecules based on the same atomic species. The fact that their general features may be shown to flow so readily from a few simple principles is of great pedagogical value in explaining the essential features of semiconductor surface science to new generations of scientists and of equally great practical value to research scientists who seek to determine the structure and properties of as yet unexplored surfaces. This article is designed to be a vehicle to provide that value to both groups of readers.

VIII. Abbreviations

1D	one dimensional
2D	two dimensional
3D	three dimensional
ARPES	angle-resolved photoemission spectroscopy
EXAFS	extended X-ray absorption fine structure
IPES	inverse photoemisssion spectroscopy
LDF	local density functional
LEED	low-energy electron diffraction
LEPD	low-energy positron diffraction
MBE	molecular beam epitaxy
RHEED	reflection high-energy electron diffraction
STM	scanning tunneling microscopy
T	temperature
UHV	ultra high vacuum

IX. Acknowledgments

I am indebted to my managers at Xerox corporation, most notably M. B. Myers, S. B. Bolte, and C. P. Holt for their continual support of my avocation of scientific research while earning a living performing other duties. Without that support this article would not have been written. I also am indebted to the numerous authors and publishers who have permitted the use herein of adaptations of their figures, and to Antoine Kahn, Dave Biegelsen, Jim Chadi and John Northrup from whom I have learned many of the things collected and articulated in this manuscript. Special thanks go to Antoine Kahn for a thorough proofreading of the manuscript and to Dan Haneman for a valuable correspondence on Si-(111) surface structures, especially the Si(111)-(5×5).

This work was supported by the sacrifices of my family and by the shareholders of Xerox Corporation without any contributions from the taxpayers of the United States of America or any other country.

X. References

(1) Duke, C. B. In *Atomic and Molecular Processing of Electronic and Ceramic Materials*; Aksay, I. A., McVay, G. L., Stroebe, T. G., Wagner, J. F., Eds.; Materials Research Society: Pittsburgh, 1987; pp 3−10.

(2) (a) Duke, C. B. *Appl. Surf. Sci.* **1993**, *65/66*, 543. (b) Duke, C. B. In *Handbook of Surface Science*; Holloway, S., Richardson, N. V., Eds; Elsevier: Amsterdam, 1996; Vol. 2, Chapter 10.

(3) (a) LaFemina, J. P.; Duke, C. B. *J. Vac. Sci. Technol. A* **1991**, *9*, 1847. (b) LaFemina, J. P. *CRC Crit. Rev. Surf. Chem* **1994**, *3*, 94.

(4) (a) Kahn, A. *Surf. Sci.* **1994,** *299/300*, 469. (b) Kahn, A. *Surf. Sci. Rep.* **1983**, *3*, 193.

(5) Duke, C. B. In *Festkörperprobleme/Adv. Solid State Phys.*; Helbig, R., Ed.; Vieweg: Breunschweig, 1994; pp 1−36.

(6) Duke, C. B. *J. Vac. Sci. Technol. B* **1993,** 11, 1336.

(7) Duke, C. B. *J. Vac. Sci. Technol. A* **1992,** 10, 2032.

(8) Schlüter, M. In *The Chemical Physics of Solid Surfaces and Heterogeneous Catalysis*; King, D. A., Woodruff, D. P., Eds.; Elsevier: Amsterdam, 1988; Vol. 5, pp 37−68.

(9) Duke, C. B. In *The Chemical Physics of Solid Surfaces and Heterogeneous Catalyis*; King, D. A. , Woodruff, D. P., Eds.; Elsevier: Amsterdam, 1988; Vol. 5, pp 64−118.

(10) Haneman, D. *Rep. Prog. Phys.* **1987**, *50*, 1045.

(11) Mönch, W. *Semiconductor Surfaces and Interfaces*, 2nd ed.; Springer Series in Surface Sciences; Springer Verlag: Berlin, 1995; Vol. 26.

(12) LaFemina, J. P. *Surf. Sci. Rep.* **1992**, 16, 133.

(13) Chadi, D. J. *Ultramicroscopy* **1989**, 31, 1.

(14) (a) Chadi, D. J. *J. Vac. Sci. Technol. A* **1987**, 5, 834. (b) Chadi, D. J. *J. Vac. Sci. Technol.* **1980**, 17, 989

(15) (a) Harrison, W. A. *J. Vac. Sci. Technol.* **1979**, 16, 1492. (b) Harrison, W. A. *J. Vac. Sci. Technol.* **1977**, *14*, 883.

(16) Martin, R. M. *J. Vac. Sci. Technol.* **1980**, *17*, 978.

(17) Farrell, H. H.; Palmstrom, C. J. *J. Vac. Sci. Technol. B* **1990**, *8*, 903. (b) Frankel, D. J.; Yu, C.; Harbison, J. P.; Farrell, H. H. *J. Vac. Sci. Technol. B* **1987**, *5*, 1113.

(18) Maclaren, J. M.; Pendry, J. B.; Rous, P. J.; Saldin, D. K., Somorjai, G. A.; Van Hove, M. A.; Vvedensky, D. D. *Surface Crystallographic Information Surface: A Handbook of Surface Structures*; D. Reidel: Dordrecht, 1987.

(19) Van Hove, M. A.; Wang, S. W.; Ogletree, D. F.; Somorjai, G. A. *Adv. Quantum Chem.* **1989**, *20*, 1.

(20) (a) Watson, P. R. *J. Phys. Chem. Ref. Data* **1992**, *21*, 123. (b) Watson, P. R. *J. Phys. Chem. Ref. Data* **1990**, *19*, 85. (c) Watson, P. R. *J. Phys. Chem. Ref. Data* **1992**, *16*, 953.

(21) Watson, P. R.; Van Hove, M. A.; Hermann, K. *NIST Surface Structure Data Base - Ver. 1*; National Institute of Standards and Technology: Gaithersburg, 1993.

(22) Unertl, W. N. In *Handbook of Surface Science*; Holloway, S., Richardson, N. V., Eds; Elsevier: Amsterdam, 1996; Vol. 2, Chapter 1.

(23) Pauling, L. *The Nature of the Chemical Bond*, 3rd ed.; Cornell University Press: Ithaca, 1960; pp 221−264.

(24) Phillips, J. C. *Bands and Bonds in Semiconductors*; Academic: New York, 1973.

(25) Chadi, D. J. In *The Structure of Surfaces III*; Tong, S. Y., Van Hove, M. A., Takayanage, K., Xie, X. D., Eds.; Springer Series in Surface Sciences; Springer Verlag: Berlin, 1991; Vol. 24, pp 532−544.

(26) (a) Pashley, M. D.; Haberern, K. W. *Phys. Rev. Lett.* **1991**, *67*, 2697. (b) Pashley, M. D.; Haberern, K. W.; Feenstra, R. M. *J. Vac. Sci. Technol. B* **1992**, *10*, 1874. (c) Pashley, M. D. In *Semiconductor Growth, Surfaces and Interfaces*; Davies, G. J., Williams, R. H., Eds.; Chapman and Hall: London, 1994; pp 91−101.

(27) (a) Zehner, D. M.; White, C. W.; Ownby, G. W. *Appl. Phys. Lett.* **1980**, *37*, 456. (b) Zehner, D. M.; White, C. W.; Ownby, G. W. *Surf. Sci.* **1980**, *90*, L67.

(28) (a) Joyce, B. A.; Dobson, P. J.; Parker, E. H. C. *In The Chemical Physics of Solid Surfaces and Heterogeneous Catalyis*; King, D. A., Woodruff, D. P., Eds.; Elsevier: Amsterdam, 1988; Vol. 5, pp 271−308. (b) Farrow, R. F. C. In *The Chemical Physics of Solid Surfaces and Heterogeneous Catalyis*; King, D. A., Woodruff, D. P., Eds.; Elsevier: Amsterdam, 1988; Vol. 5, pp 369−426.

(29) (a) Peierls, *R. E. Quantum Theory of Solids*; Clarendon Press: Oxford, 1955. (b) Chaikin, P. M. In *Synthesis and Properties of Low Dimensional Materials*; Miller, J. S., Epstein, A. J., Eds.; New York Academy of Sciences: New York, 1978; pp 128−144. (c) Mott, N. F. *Metal-Insulator Transitions*: Taylor and Francis: London, 1974. (d) Appelbaum, J. A.; Baraff, G. A.; Hamann, D. R. *Phys. Rev. Lett.* **1976**, *36*, 450.

(30) Yin, M. T.; Cohen, M. L. *Phys. Rev. B* **1981**, *24*, 2303.

(31) (a) Alerhand, O. L.; Vanderbilt, D.; Meade, R. D.; Joannopoulos, J. D. *Phys. Rev. Lett.* **1988**, *61*, 1973. (b) Vanderbilt, D.; Alerhand, O. L.; Meade, R. D.; Joannopoulos, J. D. *J. Vac. Sci. Technol. B* **1989**, *7*, 1013. (c) Alerhand, O. L.; Berker, A. N.; Joannopoulos, J. D.; Vanderbilt, D.; Hamers, R. J.; Demuth, J. E. *Phys. Rev. Lett.* **1990**, *64*, 2406.

(32) (a) Payne, M. C.; Roberts, N.; Needs, R. J.; Needels, M.; Joannopoulos, J. D. *Surf. Sci.* **1989**, *211/212*, 1. (b) Meade, R. D.; Vanderbilt, D. *Phys. Rev. Lett.* **1989**, *63*, 1404.

(33) Williams, E. D. *Surf. Sci.* **1994**, *299/300*, 502.

(34) (a) Men, F. K.; Packard, W. E.; Webb, M. B. *Phys. Rev. Lett.* **1988**, *61*, 2469. (b) Webb, M. B.; Men, F. K.; Swartzentruber, B. S.; Lagally, M. G. *J. Vac. Sci. Technol. A* **1990,** *8*, 2658.

(35) Chadi, D. J. *Phys. Rev. B* **1979**, *19*, 2074.

(36) (a) Pandey, K. C. *Phys. Rev. Lett.* **1981**, *47*, 1913. (b) Pandey, K. C. *Phys. Rev. Lett.* **1982**, *49*, 223.

(37) (a) Haneman, D.; Lagally, M. G. *J. Vac. Sci. Technol. B* **1988**, *6*, 1451. (b) Haneman, D.; Chernov, A. A. *Surf. Sci.* **1989**, *215*, 135. (c) Haneman, D.; McAlpine, N. *Phys. Rev. Lett.* **1991**, *66*, 758. (d) Chen, B.; Haneman, D. *Phys. Rev. B* **1995**, *51*, 4258.

(38) Duke, C. B.; Wang, Y. R. *J. Vac. Sci. Technol. B* **1988**, 6, 1440.

(39) Chadi, D. J. *Phys. Rev. Lett.* **1984,** *52*, 1911.

(40) (a) Tong. S. Y.; Xu, G.; Mei, W. N. *Phys. Rev. Lett.* **1984**, *52*, 1693. (b) Haberern, K. W.; Pashley, M. D. *Phys. Rev. B* **1990,** *41*, 3226.

(41) Xu, G.; Hu, W. Y.; Puga, M. W.; Tong, S. Y.; Yeh, J. L.; Wang, S. R.; Lee, B. W. *Phys. Rev. B* **1985**, *32*, 8473.

(42) Feidenhans'l, R.; Nielsen, M.; Grey, F.; Johnson, R. L.; Robinson, I. K. *Surf. Sci.* **1987,** *186*, 499.

(43) Bohr, J.; Feidenhans'l, R.; Nielsen, M.; Toney, M.; Johnson, R. L.; Robinson, I. K. *Phys. Rev. Lett.* **1985**, *54*, 1275.

(44) (a) Chadi, D. J. *Phys. Rev. Lett.* **1979**, *43*, 43. (b) Ihm, J.; Cohen, M. L.; Chadi, D. J. *Phys. Rev. B* **1980**, *21*, 4592.

(45) (a) Pashley, M. D.; Haberern, K. W.; Friday, W.; Woodall, J. M.; Kirchner, P. D. *Phys. Rev. Lett.* **1988**, *60*, 2176. (b) Biegelsen, D. K.; Bringans, R. D.; Northrup, J. E.; Swartz, L. E. *Phys. Rev. B* **1990,** *41*, 5701.

(46) (a) Biegelsen, D. K.; Bringans, R. D.; Swartz, L. E. *SPIE Proc.* **1989**, *1168*, 136. (b) Heller, E. J.; Lagally, M. G. *Appl. Phys. Lett.* **1992,** *60*, 2675. (c) Bressler-Hill, V.; Wassermeier, M.; Pond, K.; Maboudian, R.; Briggs, G. A. D.; Petroff, P. M.; Weinberg, W. H. *J. Vac. Sci. Technol. B* **1992**, *10*, 1881. (d) Xu, H.; Hashizume, T.; Sakurai, T. *Jpn. J. Appl. Phys.* **1993**, *32*, 1511.

(47) Chambers, S. A. *Surf. Sci.* **1992,** *261*, 48.

(48) Biegelsen, D. K.; Bringans, R. D.; Northrup, J. E.; Swartz, L. E. *Phys. Rev. Lett.* **1990**, *65*, 452.

(49) Takayanagi, K.; Tanishiro, Y.; Takahashi, S.; Takahashi, M. *Surf. Sci.* **1985**, 164, 367.

(50) Feidenhans'l, R.; Pederson, J. S.; Bohr, J.; Nielsen, M.; Grey, F; Johnson, R. L. *Phys. Rev. B* **1988**, *38*, 9715.

(51) Duke, C. B. *Scanning Microsc.* **1994**, *8*, 753.

(52) Vanderbilt, D. *Phys. Rev. B* **1987**, *36*, 6209.

(53) (a) Phaneuf, R. J.; Webb, M. B. *Surf. Sci.* **1985**, *164*, 167. (b) Becker, R. S.; Golovchenko, J. A.; Swartzentruber, B. S. *Phys. Rev. Lett.* **1985**, *54*, 2678.

(54) Klitsner, T.; Nelson, J. S. *Phys. Rev. Lett.* **1991**, *67*, 3800.

(55) (a) McRae, E. G.; Malic, R. A. *Phys. Rev. Lett.* **1987**, *58*, 1437. (b) McRea, E. G.; Malic, R. A. *Phys. Rev. B* **1988**, *38*, 13163. (c) Feenstra, R. M.; Slavin, A. J.; Held, G. A.; Lutz, M. A. *Phys. Rev. Lett.* **1991**, *66*, 3257. (d) Denier van der Gon, A. W.; Gay, J. M.; Frenken, J. W. M.; van der Veen, J. F. *Surf. Sci.* **1991**, *241*, 335. (e) Patthey, L.; Bullock, E. L.; Hricovini, K. *Surf. Sci.* **1992**, *269/270*, 28. (f) Feenstra, R. M.; Slavin, A. J.; Held, G. A.; Lutz, M. A. *Ultramicroscopy* **1992**, *42−44*, 33. (g) Feenstra, R. M.; Held, G. A. *Physica D* **1993**, *66*, 43.

(56) (a) Appelbaum, J. A.; Baraff, G. A.; Hamann, D. R. *Phys. Rev. B* **1976,** *14*, 1623. (b) Ludeke, R. *Phys. Rev. Lett.* **1977**, *39*, 1042. (c) Farrell, H. H.; Harbison, J. P.; Peterson, L. D. *J. Vac. Sci. Technol. B* **1987,** *5*, 1482. (d) Pashley, M. D. *Phys. Rev. B* **1989**, *40*, 10481.

(57) Chen, W.; Dumas, M.; Mao, D.; Kahn, A. *J. Vac. Sci. Technol. B* **1992,** *10*, 1886.

(58) Dassanayake, U. M.; Chen, W. Kahn, A. *J. Vac. Sci. Technol. B* **1993**, *11*, 1467.

(59) Sung, M. M.; Kim, C.; Bu, H.; Karpuzov, D. S.; Rabalais, J. W. *Surf. Sci.* **1995**, *322*, 116.

(60) (a) Northrup, J. E.; Froyen, S. *Phys. Rev. Lett.* **1993**, *71*, 2276. (b) Northrup, J. E.; Froyen, S. Phys. *Rev. B* **1994**, *50*, 2015.

(61) Gray, H. B. *Electrons and Chemical Bonding*; Benjamin: New York, 1965; pp 155−175.

(62) Duke, C. B. *J. Vac. Sci. Technol. B* **1983**, *1*, 732.

(63) Godin, T. J.; LaFemina, J. P.; Duke, C. B. *J. Vac. Sci. Technol. A* **1992**, *10*, 2059.

(64) (a) Stich, I.; Payne, M. C.; King-Smigh, R. D.; Lin, J.-S.; Clarke, L. J. *Phys. Rev. Lett.* **1992**, *68*, 1351. (b) Brommer, K. D.; Needles, M.; Larson, B. E.; Joannopoulos, J. D. *Phys. Rev. Lett.* **1992**, *68*, 1355. (c) Needels, M. *Phys. Rev. Lett.* **1993,** *71*, 3612. (d) Stich, I.; Payne, M. C.; King-Smith, R. D.; Lin, J. S.; Clarke, L. J.; Brommer, K. D.; Joannopoulos, J. D.; Larson, B. E. *Phys.*

Rev. Lett. **1993**, *71*, 3613. (e) Brommer, K. D.; Galván, M.; Dal Pino, A., Jr.; Joannopoulos, J. D. *Surf. Sci.* **1994**, *314*, 57.
(65) Dabrowski, J.; Scheffler, M. *Appl. Surf. Sci.* **1992**, *56*−58, 15.
(66) Kruger, P.; Pollmann, J. *Phys. Rev. B* **1993**, *47*, 1898.
(67) (a) Mailhiot, C.; Duke, C. B.; Chadi, D. J. *Phys. Rev. B* **1985**, *31*, 2213. (b) Duke, C. B.; Wang, Y. R. *J. Vac. Sci. Technol. A* **1989**, *7*, 2035.
(68) Duke, C. B.; Wang, Y. R. *J. Vac. Sci. Technol. A* **1988**, *6*, 692.
(69) (a) Pandey, K. C. *Phys. Rev. Lett.* **1981**, *47*, 1913. (b) Pandey, K. C. *Phys. Rev. Lett.* **1982**, *49*, 223.
(70) (a) Himpsel, F. J.; Marcus, P. M.; Tromp, R.; Batra, I. P.; Cook, M. R.; Jona, F.; Liu, H. *Phys. Rev. B* **1984**, *30*, 2257. (b) Sakama, H; Kawazu, A; Ueda, K. *Phys. Rev. B* **1986,** *34*, 1367.
(71) Smit, L.; Tromp, R. M.; Van Der Veen, J. F. *Surf. Sci.* **1985**, *163*, 315.
(72) Northrup, J. E.; Hybertsen, M. S.; Louie, S. G. *Phys. Rev. Lett.* **1991**, *66*, 500.
(73) (a) Northrup, J. E.; Cohen, M. L. *Phys. Rev. Lett.* **1982**, *49*, 1349. (b) Northrup, J. E.; Cohen, M. L. *J. Vac. Sci. Technol.* **1982**, *21*, 333. (c) Northrup, J. E.; Cohen, M. L. *Phys. Rev. B* **1983**, *27*, 6553.
(74) (a) Stroscio, J. A.; Feenstra, R. M.; Fein, A. P. *J. Vac. Sci. Technol. A* **1987**, *5*, 838. (b) Feenstra, R. M.; Stroscio, J. A. *Phys. Script.* **1987,** *T19*, 55.
(75) Tong, S. Y.; Huang, H.; Wei, C. M.; Packard, W. E.; Men, F. K.; Glander, G.; Webb, M. B. *J. Vac. Sci. Technol. A* **1988,** *6*, 615.
(76) Robinson, I. K.; Waskiewicz, W. K.; Fuoss, P. H.; Stark, J. B.; Bennett, P. A. *Phys. Rev. B* **1986**, *33*, 7013.
(77) Robinson, I. K.; Vlieg, E. *Surf. Sci.* **1992,** *261*, 123
(78) Twesten, R. D., Gibson, J. M. *Ultramicroscopy* **1994**, *53*, 223.
(79) Tromp, R. M.; Hamers, R. J.; Demuth, J. E. *Phys. Rev. B* **1986,** *34*, 1388.
(80) (a) Ichimiya, A. *Surf. Sci.* **1987**, *192*, L893. (b) Ma, Y.; Lordi, S.; Eades, J. A. *Surf. Sci.* **1994**, *313*, 317. (c) Ma, Y.; Lordi, S.; Eades, J. A.; Ino, S. *Phys. Rev. B* **1994,** *49*, 17448. (d) Hanada, T.; Ino, S.; Daimon, H. *Surf. Sci.* **1994,** *313*, 143.
(81) Qian, G. X.; Chadi, D. J. *Phys. Rev. B* **1987**, *35*, 1288.
(82) Feenstra, R. M.; Lutz, M. A. *Surf. Sci.* **1991**, *243*, 151.
(83) (a) Ihm, J.; Lee, D. H.; Joannopoulos, J. D.; Xiong, J. J. *Phys. Rev. Lett.* **1983,** *51*, 1872. (b) Saxena, A; Gawlinski, E. T.; Gunton, J. D. *Surf. Sci.* **1985**, *160*, 618.
(84) Hamers, R. J.; Tromp, R. M.; Demuth, J. E. *Phys. Rev. B* **1986**, *34*, 5343.
(85) Uhrberg, R. I. G.; Hanson, G. V. *Crit. Rev. Solid State Mater. Sci.* **1991**, *17*, 133.
(86) Krüger, P.; Pollmann, J. *Phys. Rev. Lett.* **1995**, *74*, 1155.
(87) Jayaram, G.; Xu, P.; Marks, L. D. *Phys. Rev. Lett.* **1993**, *71*, 3489.
(88) Shkrebtii, A. I.; Del Sole, R. *Phys. Rev. Lett.* **1993,** *70*, 2645.
(89) Wolkow, R. A. *Phys. Rev. Lett.* **1992**, *68*, 2636.
(90) (a) Munz, A. W.; Ziegler, Ch.; Göpel, W. *Phys. Rev. Lett.* **1995**, *74*, 2244. (b) Molotov, S. N.; Nazin, S. S.; Smirnova, I. S.; Tatarskii, V. V. *Surf. Sci.* **1991**, *259*, 339.
(91) (a) Landemark, E.; Karlsson, C. J.; Chao, Y. C.; Uhrberg, R. I. G. *Phys. Rev. Lett.* **1992**, *69*, 1588. (b) Bullock, E. L.; Gunnella, R.; Patthey, L.; Abukawa, T.; Kono, S.; Natoli, C. R.; Johansson, L. S. O. *Phys. Rev. Lett.* **1995,** *74*, 2756. (c) Wertheim, G. K.; Riffe, D. M.; Rowe, J. E.; Citrin, P. H.; *Phys. Rev. Lett.* **1991**, *67*, 120.
(92) Tabata, T.; Argu, T.; Murata, Y. *Surf. Sci.* **1987**, *179*, L63.
(93) Badt, D.; Wengelnik, H.; Neddermeyer, H. *J. Vac. Sci. Technol. B* **1994**, *12*, 2015.
(94) Northrup, J. E. *Phys. Rev. B* **1993**, *47*, 10032.
(95) Johansson, L. S. O.; Uhrberg, R. I. G.; Martensson, P.; Hansson, G. V. *Phys. Rev. B* **1990,** *42*, 1305.
(96) Enta, Y.; Suzuki, S.; Kono. S. *Phys. Rev. Lett.* **1990,** *65*, 2704.
(97) (a) Shu, Z.; Shima, N.; Tsukada, M. *Phys. Rev. B* **1989**, *40*, 11868. (b) Low, K. C.; Ono, C. K. *Phys. Rev. B* **1994**, *50*, 5352. (c) Gryko, J.; Allen, R. E. *Physica B* **1994**, *194*−196, 381. (d) Shkrebtii, A. I.; Di Felice, R.; Bertoni, C. M.; Del Sole, R. *Phys. Rev. B* **1995,** *51*, 11201.
(98) (a) Garcia, A.; Northrup, J. E. *Phys. Rev. B* **1993**, *48*, 17350. (b) Dabrowski, J.; Pehlke, E.; Scheffler, M. *Phys. Rev. B* **1994**, *49*, 4790. (c) Roberts, N.; Needs, R. J. *Surf. Sci.* **1990**, *236*, 112.
(99) Grazhulis, V. A. *Appl. Surf. Sci.* **1988,** *33/34*, 1.
(100) Northrup, J. E.; Cohen, M. L. *Phys. Rev. B* **1983**, *27*, 6553.
(101) Nicholls, J. M.; Hansson, G. V.; Uhrberg, R. I. G.; Flodström, S. A. *Phys. Rev. B* **1983**, *27*, 2594.
(102) Zhu, X.; Louie, S. G. *Phys. Rev. B* **1991**, *43*, 12146.
(103) (a) Nicholls, J. M.; Hansson, G. V.; Karlsson, U. O.; Uhrberg, R. I. G.; Engelhardt, R.; Seki, K.; Flodström, S. A.; Koch, E. E. *Phys. Rev. Lett.* **1984**, *52*, 1555. (b) Solal, F.; Jezequel, G.; Barski, A.; Steiner, P.; Pinchaux, R.; Petroff, Y. *Phys. Rev. Lett.* **1984,** *52*, 360.
(104) Nicholls, J. M.; Reihl, B. *Surf. Sci.* **1989**, *218*, 237.
(105) Takeuchi, N.; Selloni, A.; Shkrebtii, A. I.; Tosatti, E. *Phys. Rev. B* **1991**, *44*, 13611.
(106) Takeuchi, N.; Selloni, A.; Tosatti, E. *Phys. Rev. B* **1995** *51*, 10844.
(107) Aarts, J.; Hoeven, A. J.; Larsen, P. K. *Phys. Rev. B* **1988**, *37*, 8190.
(108) Becker, R. S.; Swartzentruber, B. S.; Vickers, J. S.; Klitsner, T. *Phys. Rev. B* **1989**, *39*, 1633.
(109) Hirschorn, E. S.; Lin, D. S.; Leibsle, F. M.; Samsavar, A.; Chiang, T.-C. *Phys. Rev. B* **1991**, *44*, 1403.
(110) Marée, P. J. M.; Nakagawa, K.; Van der Veen, J. F.; Tromp, R. M. *Phys. Rev. B* **1988**, *38*, 1585.
(111) Tong, S. Y.; Huang, H.; Wei, C. M. In *Chemistry and Physics of Solid Surfaces*; Vaneslow, R., Howe, R., Eds.; Springer Verlag: Berlin, 1990; Vol. 8, pp 395−417.
(112) Van Silfhout, R. G.; Van der Veen, J. F.; Norris, C.; Macdonald, J. E. *Faraday Discuss. Chem. Soc.* **1990**, *89*, 169.
(113) (a) Feenstra, R. M.; Slavin, A. J. *Surf. Sci.* **1991**, *251/252*, 401. (b) Bouchard, A. M.; Osbourn, G. C.; Swartzentruber, B. S. *Surf. Sci.* **1994**, *321*, 276.
(114) Le Lay, G.; Kanski, J.; Nilsson, P. O.; Karlsson, U. O.; Hricovini, K. P. *Phys. Rev. B* **1992**, *45*, 6692.
(115) Lambert, W. R.; Trevor, P. L.; Cardillo, M. J.; Sakai, A.; Hamann, D. R. *Phys. Rev. B* **1987**, *35*, 8055.
(116) Culbertson, R. J.; Kuk, Y.; Feldman, L. C. *Surf. Sci.* **1986,** *167*, 127.
(117) Grey, F.; Johnson, R. l.; Skov Petersen, J.; Feidenhans'l, R.; Nielsen, M. In *The Structure of Surfaces II*; Van der Veen, J. F., Van Hove, M. A., Eds.; Springer Series in Surface Sciences; Springer Verlag: Berlin, 1988; Vol. 11, pp 292−297.
(118) Kubby, J. A.; Griffith, J. E.; Becker, R. S.; Vickers, J. S. *Phys. Rev. B* **1987,** *36*, 6079.
(119) Rossmann, R.; Meyerheim, H. L.; Jahns, V.; Wever, J.; Moritz, W.; Wolf, D.; Dornisch, D.; Schulz, H. *Surf. Sci.* **1992,** *279*, 199.
(120) Mitome, M.; Takayanagi, K. *Surf. Sci.* **1991**, *242*, 69.
(121) Johnson, A. D.; Norris, C.; Frenken, J. W. M.; Derbyshire, H. S.; MacDonald, J. E. *Phys. Rev. B* **1991**, *44*, 1134.
(122) Lucas, C. A.; Dower, C. S.; McMorrow, D. F.; Wong, G. C. L.; Lamelas, F. J.; Fuoss, P. H. *Phys. Rev. B* **1993**, *47*, 10375.
(123) (a) Needles, M.; Payne, M. C.; Joannopoulos, J. D. *Phys. Rev. Lett.* **1987**, *58*, 1765. (b) Needles, M.; Payne, M. C.; Joannopoulos, J. D. *Phys. Rev. B* **1988,** *38*, 5543.
(124) Spiess, L.; Freeman, A. J.; Soukiassian, P. *Phys. Rev. B* **1994**, *50*, 2249.
(125) (a) Zandvliet, H. J. W.; Terpstra, D.; Van Silfhout, A. *J. Phys.: Condens. Matter* **1991**, *3*, 409. (b) Zandvliet, H. J. W.; Caspers, W. J.; Van Silfhout, A. *Solid State Commun.* **1991**, *78*, 455.
(126) (a) Krüger, P.; Mazur, A.; Pollmann, J.; Wolfgarten, G. *Phys. Rev. Lett.* **1986**, *57*, 1468. (b) Pollmann, J.; Krüger, P.; Mazur, A. *J. Vac. Sci. Technol. B* **1987**, *5*, 945.
(127) Landemark, E.; Uhrberg, R. I. G.; Krüger, P.; Pollmann, J. *Surf. Sci.* **1990,** *236*, L359.
(128) Duke, C. B.; Wang, Y. R. *J. Vac. Sci. Technol. B* **1989**, *7*, 1027.
(129) (a) Zhu, X.; Zhang, S. B.; Louie, S. G.; Cohen, M. L. *Phys. Rev. Lett.* **1989**, *63*, 2112. (b) Manghi, F.; Molinari, E.; Selloni, A.; Del Sole, R. *Phys. Rev. Lett.* **1990**, *65*, 937. (c) Zhu, X.; Zhang, S. B.; Louie, S. G.; Cohen, M. L. *Phys. Rev. Lett.* **1990,** *65*, 938.
(130) (a) Alves, J. L. A.; Hebenstreit, J.; Scheffler, M. *Phys. Rev. B* **1991**, *44*, 6188. (b) Jenkins, S. J.; Srivastava, G. P.; Inkson, J. C. *Surf. Rev., Lett.* **1994**, *1*, 473.
(131) Huijser, A.; Van Laar, J.; Van Rooy, T. L. *Phys. Lett.* **1978,** *65A*, 337.
(132) Haight, R.; Silberman, J. A. *Phys. Rev. Lett.* **1989**, *62*, 815.
(133) Straub, D.; Skibowski, M.; Himpsel, F. J. *Phys. Rev. B* **1985**, *32*, 5237.
(134) Reihl, B.; Riesterer, T.; Tschudy, M.; Perfetti, P. *Phys. Rev. B* **1988**, *38*, 13456.
(135) Lessor, D. L.; Duke, C. B.; Kahn, A.; Ford, W. K. *J. Vac. Sci. Technol. A* **1993**, *11*, 2205.
(136) Klepeis, J. E.; Mailhiot, C.; Van Schlifgaarde, M.; Methfessel, M. *J. Vac. Sci. Technol. A* **1993**, *11*, 1463.
(137) Kendelewicz, T.; Klepeis, J. E.; Woicik, J. C.; Southworth, S. H.; Mailhiot, C.; Van Schilfgaarde, M.; Methfessel, M.; Herrera-Gomez, A.; Miyano, K. E. *Phys. Rev. B* **1995**, *51*, 10774.
(138) Wang, Y. R.; Duke, C. B.; Magnusson, K. O.; Flodström, S. A. *Surf. Sci.* **1988**, *205*, L760.
(139) (a) Alves, J. L. A.; Watari, K.; Ferraz, A. C. *Solid State Commun.* **1993,** *87*, 1001. (b) Ferraz, A. C.; Alves, J. L. A.; Watari, K. *Surf. Sci.* **1994**, *307*−309, 959. (c) Alves, J. L. A.; Watari, K.; Ferraz, A. C. *Braz. J. Phys.* **1994**, *24*, 99.
(140) Chen, X. M.; Canter, K. F.; Duke, C. B.; Paton, A.; Lessor, D. L; Ford, W. K. *Phys. Rev. B* **1993**, *48*, 2400.
(141) Joly, Y. *Phys. Rev. Lett.* **1994**, *72*, 392.
(142) Wang, J.; Arias, T. A.; Joannopoulos, J. D.; Turner, G. W.; Alerhand, O. L. *Phys. Rev. B* **1993**, *47*, 10326.
(143) Ruocco, A.; Biagini, M.; Di Bona, A.; Gambacorti, N.; Valeri, S.; Nannarone, S.; Santoni, A.; Bonnet, J. *Phys. Rev. B* **1995**, *51*, 2399.
(144) (a) Ebert, Ph.; Cox, G.; Poppe, U.; Urban, K. *Surf. Sci.* **1992**, 271, 587. (b) Ebert, Ph.; Cox, G.; Poppe, U.; Urban, K. *Ultramicroscopy* **1992**, *42*−44, 871.
(145) Woicik, J. C.; Kendelewicz, T.; Miyano, K. E.; Cowan, P. L.; Bouldin, C. E.; Karlin, B. A.; Pianetta, P.; Spicer, W. E. *Phys. Rev. Lett.* **1992**, *68*, 341.
(146) (a) Woicik, J. C.; Kendelewicz, T.; Miyano, K. E.; Richter, M.; Bouldin, C. E.; Pianetta, P.; Spicer, W. E. *Phys. Rev. B* **1992**, *46*, 9869. (b) Mangat, P. S.; Kim, S. T.; Choudhary, K. M.; Hurych, Z.; Soukiassian, P. *Surf. Sci.* **1993**, *285*, 102.

(147) Gota, S.; Gunnella, R.; Wu, Z.-Y.; Jézéquel, G.; Natoli, C. R.; Sébilleau, D.; Bullock, E. L.; Proix, F.; Guillot, C.; Quémerais, A. *Phys. Rev. Lett.* **1993**, *71*, 3387.
(148) Kahn, A.; Duke, C. B.; Paton, A. *Phys. Rev. B* **1991**, *44*, 5606.
(149) (a) Duke, C. B.; Paton, A.; Wang, Y. R.; Stiles, K.; Kahn, A. *Surf. Sci.* **1988**, *197*, 11. (b) Duke, C. B.; Paton, A.; Wang, Y. R.; Stiles, K.; Kahn, A. *Surf. Sci.* **1989**, *214*, 334. (c) Duke, C. B.; Paton, A.; Wang, Y. R.; Stiles, K.; Kahn, A. *Surf. Sci.* **1989**, *221*, 619.
(150) Wang, Y. R.; Duke, C. B.; Stevens, K.; Kahn, A.; Magnusson, K. O.; Flodström, S. A. *Surf. Sci.* **1988**, *206*, L817.
(151) (a) Schröer, P.; Krüger, P.; Pollmann, J. *Phys. Rev. B* **1994**, *49*, 17092. (b) Schröer, P.; Krüger, P.; Pollmann, J. In *Proceedings of the Fourth International Conference on the Formation of Semiconductor Interfaces*; Langeler, B., Luth, H., Mönch, W., Pollmann, J., Eds.; World Scientific: Singapore, 1994; pp 85−88.
(152) Jaffe, J. E.; Harrison, N. M.; Hess, A. C. *Phys. Rev. B* **1994**, *49*, 11153.
(153) Martins, J. B. L.; Moliner, V.; Andres, J.; Longo, E.; Taft, C. A. *J. Mol. Struct.* **1995**, *330*, 347.
(154) Horsky, T. N.; Brandes, G. R.; Canter, K. F.; Duke, C. B.; Paton, A.; Lessor, D. L.; Kahn, A.; Horng, S. F.; Stevens, K.; Stiles, K.; Mills, A. P., Jr. *Phys. Rev. B* **1992**, *46*, 7011.
(155) Wang, Y. R.; Duke, C. B. *Surf. Sci.* **1987**, *192*, 309.
(156) Wang, Y. R.; Duke, C. B. *Phys. Rev. B* **1988**, *37*, 6417.
(157) (a) Canter, K. F.; Duke, C. B.; Mills, A. P., Jr. In *Chemistry and Physics of Solid Surfaces*; Vaneslow, R., Howe, R., Eds.; Springer Verlag: Berlin, 1990; Vol. 8, pp 183−211. (b) Duke, C. B. In *Positron Spectroscopy of Solids, Proceedings of the International School of Physics 'Enrico Fermi' Course CXXV*; Dupasquier, A., Mills, A. P., Jr., Eds.; IOS Press: Amsterdam, 1995; pp 317−359.
(158) Thornton, J. M. C.; Unsworth, P.; Jackson, M. D.; Weightman, P.; Woolf, D. A. *Surf. Sci.* **1994**, *316*, 231.
(159) Ranke, W.; Jacobi, K. *Surf. Sci.* **1977**, *63*, 33.
(160) (a) Kaxiras, E.; Bar-Yam, Y.; Joannopoulos, J. D.; Pandey, K. C. *Phys. Rev. B* **1987,** *35*, 9625. (b) Kaxiras, E.; Bar-Yam, Y.; Joannopoulos, J. D.; Pandey, K. C. *Phys. Rev. B* **1987**, *35*, 9636.
(161) Chetty, N.; Martin R. M. *Phys. Rev. B* **1992**, *45*, 6089.
(162) Chadi, D. J. *J. Vac. Sci. Technol. A* **1986**, *4*, 944.
(163) (a) Fu, J.; Kim, J.; Gallagher, M. C.; Willis, R. F.; Miller, D. L. *Surf. Sci.* **1994**, *318*, 349. (b) Kim, J.; Gallagher, M. C.; Willis, R. F.; Fu, J.; Miller, D. L. *J. Vac. Sci. Technol. A* **1994**, *12*, 2145.
(164) Nakada, T.; Osaka, T. *Phys. Rev. Lett.* **1991**, *67*, 2834.
(165) Ping, J. G.; Ruda, H. E. J. *Appl. Phys.* **1994**, *75*, 5332.
(166) Hashizume, T.; Xue, Q. K.; Zhou, J.; Ichimiya, A.; Sakurai, T. *Phys. Rev. Lett.* **1994**, *73*, 2208.
(167) Xue, Q.; Hashizume, T.; Zhou, J. M.; Sakata, T.; Ohno, T.; Sakurai, T. *Phys. Rev. Lett.* **1995**, *74*, 3177.
(168) Chadi, D. J. *J. Vac. Sci. Technol. A* **1987**, *5*, 834.
(169) (a) Farrell, H. H.; Palmstrøm, C. J. *J. Vac. Sci. Technol. B* **1990**, *8*, 903. (b) Farrell, H. H.; Harbison, J. P.; Peterson, L. D. *J. Vac. Sci. Technol. B* **1987**, *5*, 1482.
(170) (a) Qian, G.-X.; Martin, R. M.; Chadi, D. J. *Phys. Rev. B* **1988**, *38*, 7649. (b) Qian, G.-X.; Martin, R. M.; Chadi, D. J. *J. Vac. Sci. Technol. B* **1987,** *5*, 933.
(171) Ohno, T. *Phys. Rev. Lett.* **1993**, *70*, 631.
(172) Heller, E. J.; Shang, Z. Y.; Lagally, M. G. *Phys. Rev. Lett.* **1993**, *71*, 743.
(173) Skala, S. L.; Hubacek, J. S.; Tucker, J. R.; Lyding, J. W.; Chou, S. T.; Cheng, K.-Y. *Phys. Rev. B* **1993**, *48*, 9138.
(174) Falta, J.; Tromp, R, M.; Copel, M.; Pettit, G. D.; Kirchner, P. D. *Phys. Rev. Lett.* **1992**, *69*, 3068.
(175) Pashley, M. D. *Phys. Rev. Lett.* **1993**, *70*, 3171.
(176) Sauvage-Simkin, M.; Pinchaux, R.; Massies, J.; Calverie, P.; Jedrecy, N.; Bonnet, J.; Robinson, I. K. *Phys. Rev. Lett.* **1989,** *62*, 563.
(177) Xu, C.; Caffey, K. P.; Burnham, J. S.; Goss, S. H.; Garrison, B. J.; Winograd, N. *Phys. Rev. B* **1992**, *45*, 6776.
(178) Cerdá, J.; Palomares, F. J.; Soria, F. *Phys. Rev. Lett.* **1995**, *75*, 665.
(179) Schweitzer, M. O.; Leibsle, F. M.; Jones, T. S.; McConville, C. F.; Richardson, N. V. *Surf. Sci.* **1993**, *280*, 63.

CR950212S